# Improved analysis of $J/\psi$ decays into a vector meson and two pseudoscalars

Timo A. Lähde[1,*] and Ulf-G. Meißner[1,2,†]

[1]*Helmholtz-Institut für Strahlen- und Kernphysik (HISKP), Bonn University, Nußallee 14-16, D-53115 Bonn, Germany*
[2]*Forschungszentrum Jülich, Institut für Kernphysik (Th), D-52425 Jülich, Germany*

(Received 12 June 2006; published 28 August 2006)

Recently, the BES collaboration has published an extensive partial-wave analysis of experimental data on $J/\psi \to \phi\pi^+\pi^-$, $J/\psi \to \omega\pi^+\pi^-$, $J/\psi \to \phi K^+K^-$ and $J/\psi \to \omega K^+K^-$. These new results are analyzed here, with full account of detection efficiencies, in the framework of a chiral unitary description with coupled-channel final state interactions between $\pi\pi$ and $K\bar{K}$ pairs. The emission of a dimeson pair is described in terms of the strange and nonstrange scalar form factors of the pion and the kaon, which include the final state interaction and are constrained by unitarity and by matching to the next-to-leading-order chiral expressions. This procedure allows for a calculation of the $S$-wave component of the dimeson spectrum including the $f_0(980)$ resonance, and for an estimation of the low-energy constants of Chiral Perturbation Theory, in particular, the large $N_c$ suppressed constants $L_4^r$ and $L_6^r$. The decays in question are also sensitive to physics associated with OZI violation in the $0^{++}$ channel. It is found that the $S$-wave contributions to $\phi\pi^+\pi^-$, $\phi K^+K^-$ and $\omega\pi^+\pi^-$ given by the BES partial-wave analysis may be very well fitted up to a dimeson center-of-mass energy of $\sim$1.2 GeV, for a large and positive value of $L_4^r$ and a value of $L_6^r$ compatible with zero. An accurate determination of the amount of OZI violation in the $J/\psi \to \phi\pi^+\pi^-$ decay is achieved, and the $S$-wave contribution to $\omega K^+K^-$ near threshold is predicted.

DOI: 10.1103/PhysRevD.74.034021 PACS numbers: 13.20.Gd, 12.39.Fe

## I. INTRODUCTION

The decays of the $J/\psi$ into a vector meson such as $\phi$ or $\omega$, via emission of a pair of light pseudoscalar mesons, may yield insight into the dynamics of the pseudo-Goldstone bosons of QCD [1–3], and, in particular, into the final state interaction (FSI) between $\pi\pi$ and $K\bar{K}$ pairs, which is an essential component in a realistic description of the scalar form factors (FFs) of pions and kaons. Additionally, such decays can yield insight into violation of the Okubo-Zweig-Iizuka (OZI) rule [4–6] in the scalar ($0^{++}$) sector of QCD, since the leading order contributions to such decays are OZI suppressed. Furthermore, as shown in Fig. 1, a doubly OZI-violating component may contribute to these $J/\psi$ decays, which was demonstrated already in Refs. [7,8] although the data from the DM2 [9], MARK-III [10] and BES [11] collaborations available at that time had rather low statistics. However, since then the BES collaboration has published far superior data on $J/\psi \to \phi\pi^+\pi^-$ and $J/\psi \to \phi K^+K^-$ [12], as well as for $J/\psi \to \omega\pi^+\pi^-$ and $J/\psi \to \omega K^+K^-$ [13,14]. Additionally, a comprehensive partial-wave analysis (PWA) has been performed for those data, which is particularly significant since an explicit determination of the $S$-wave $\pi\pi$ and $K\bar{K}$ event distributions is thus available. Thus, a much more precise analysis of the issues first touched upon in Ref. [7] is clearly called for.

A key ingredient in such an analysis is a realistic treatment of the final state interaction (FSI). It has been demonstrated in Ref. [15] that the FSI in the $\pi\pi$–$K\bar{K}$ system can be well described by a coupled-channel Bethe-Salpeter approach using the lowest order CHPT amplitudes for meson-meson scattering [16–18]. In such an approach, the lowest resonances in the $0^{++}$ sector are of dynamical origin, i.e. they arise due to the strong rescattering effects in the $\pi\pi$ or $K\bar{K}$ system. Such dynamically generated states include the $\sigma$ and $f_0(980)$ mesons, which are prominent in the BES data on dimeson emission from the $J/\psi$ [12–14]. It is useful, in view of the controversial nature of the $f_0(980)$ [1–3,19–22], to recall Ref. [23], which generalizes the work of Ref. [15]. There, explicit $S$-wave

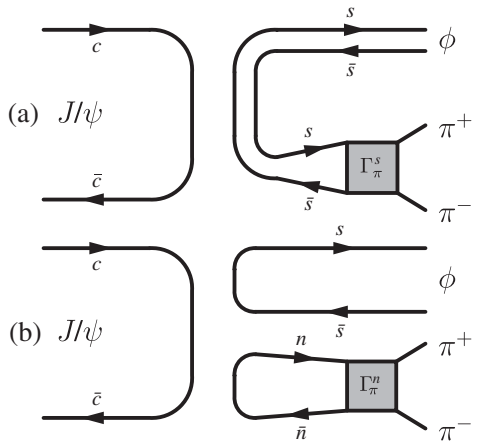


FIG. 1. Quark line diagrams for the decay of a $J/\psi$ into a light vector meson ($\phi$) and a pair of light pseudoscalar mesons ($\pi^+\pi^-$). The annihilation of the $c\bar{c}$ pair proceeds via at least three gluons. The shaded squares denote the strange ($\Gamma_\pi^s$) and nonstrange ($\Gamma_\pi^n$) scalar FFs of the pion. Note that diagram (b) is further OZI-suppressed with respect to diagram (a).

*Electronic address: talahde@pcu.helsinki.fi
†Electronic address: meissner@itkp.uni-bonn.de

 

resonance exchanges were included together with the lowest order CHPT contributions in a study of the partial-wave amplitudes for the whole scalar sector with $I = 0, 1/2$ and 1. It was noted that the results of Ref. [15] could be recovered when the explicit tree-level resonance contributions were dropped. The conclusion of Ref. [23] was that the lowest nonet of scalar resonances, which includes the $\sigma$, $\kappa$ and $a_0(980)$ states, is of dynamical origin, while a preexisting octet of scalar resonances is present at $\sim$1.4 GeV. It was also noted that the physical $f_0(980)$ state obtains a strong contribution of dynamical origin, and may also receive one from a preexisting singlet state.

This analysis uses the formalism introduced in Ref. [7], where the expressions for the scalar FFs of the pions and kaons were obtained using the results of Ref. [15]. This allows for a description of the scalar FFs which takes into account the FSI between pions and kaons up to $\sim$1.2 GeV. At higher energies, a number of preexisting scalar resonances such as the $f_0(1500)$ have to be accounted for, as well as the effects of multiparticle intermediate states, most importantly the $4\pi$ state. These scalar FFs may then be constrained by matching to the next-to-leading-order (NLO) chiral expressions. This allows for a fit of the large $N_c$ suppressed Low-Energy Constants (LECs) $L_4^r$ and $L_6^r$ of CHPT to the dimeson spectra of the $J/\psi \to \phi\pi\pi$ and $J/\psi \to \phi K\bar{K}$ decays, using the Lagrangian model of Ref. [7]. The amount of direct OZI violation present in these decays may also be accurately estimated. Finally, it should be noted that the present treatment of the FSI has been proven successful in describing, in the same spirit, a wide variety of processes, such as the photon fusion reactions $\gamma\gamma \to \pi\pi$ and $\gamma\gamma \to K\bar{K}$ [24], the decays $\phi \to \gamma\pi\pi$ and $\phi \to \gamma K\bar{K}$ [25], and more recently the hadronic decays $D, D_s \to \pi\pi\pi$ and $D, D_s \to K\pi\pi$ [26].

This paper is organized in the following manner: In Sec. II the description of the $J/\psi \to \phi\pi\pi$ decays is briefly reviewed, along with the FSI in the $\pi\pi$–$K\bar{K}$ system, as applied to the scalar FFs of the pseudo-Goldstone bosons. Some minor corrections to the NLO CHPT expressions in Ref. [7] are also pointed out. Sec. III describes the analysis of the experimental BES data, along with a discussion of the fitted parameter values, with emphasis on the LECs of CHPT and the evidence for OZI violation. In Sec. IV, the results are summarized along with a concluding discussion.

## II. THEORETICAL FRAMEWORK

The theoretical tools required for the calculation of the scalar FFs of the pseudo-Goldstone bosons using CHPT and unitarity constraints have, as discussed in the Introduction, already been extensively treated in the existing literature, and therefore only the parts directly relevant to the present analysis are repeated here. For convenience, the NLO expressions for the scalar FFs of the pseudo-Goldstone bosons are explicitly given here. Also, the expressions for the scalar FFs of the pion in Ref. [7] require a minor correction,[1] such that an updated version is called for. A derivation of the scalar FFs using unitarity and the methods of Ref. [15] is given in Ref. [7], and introductions to CHPT can e.g. be found in Ref. [27].

### A. Amplitude for $\pi\pi$ and $K\bar{K}$ emission

This work makes use of the SU(3) and Lorentz invariant Lagrangian of Ref. [7] to describe the decay of a $J/\psi$ into a pair of pseudoscalar mesons and a light vector meson, as illustrated in Fig. 2. This Lagrangian can be written as

$$\mathcal{L} = g\Psi_\mu(\langle \mathcal{V}_8^\mu \Sigma_8 \rangle + \nu \mathcal{V}_1^\mu \Sigma_1), \tag{1}$$

where the $\mathcal{V}_8$ and $\mathcal{V}_1$ denote the lowest octet and singlet of vector meson resonances. Similarly, the $\Sigma_8$ and $\Sigma_1$ refer to the corresponding sets of scalar sources, as defined in Ref. [7]. In the above equation, $g$ denotes a coupling constant, the precise value of which is not required in the present analysis, while the real parameter $\nu$ will be shown to play the role of an OZI violation parameter in the $\phi\pi^+\pi^-$ channel. Furthermore, the angled brackets in Eq. (1) denote the trace with respect to the SU(3) indices of the matrices $\mathcal{V}_8$ and $\Sigma_8$. Evaluation of that trace yields

$$\mathcal{L} = g\Psi_\mu(V_8^\mu S_8 + \nu \mathcal{V}_1^\mu \Sigma_1 + \cdots), \tag{2}$$

where only the terms relevant for the present considerations have been written out. Here $V_8$ denotes the $I = 0$ state of the octet of vector meson resonances, while $S_8$ again refers to the corresponding operator in the matrix of scalar sources. The $\phi$ and $\omega$ fields, along with the associated scalar sources $S_\phi$ and $S_\omega$ are then introduced according to

$$V_8 = \frac{\omega}{\sqrt{3}} - \sqrt{\frac{2}{3}}\phi, \qquad S_8 = \frac{S_\omega}{\sqrt{3}} - \sqrt{\frac{2}{3}}S_\phi, \tag{3}$$

$$\mathcal{V}_1 = \sqrt{\frac{2}{3}}\omega + \frac{\phi}{\sqrt{3}}, \qquad \Sigma_1 = \sqrt{\frac{2}{3}}S_\omega + \frac{S_\phi}{\sqrt{3}}, \tag{4}$$

which corresponds to the ansatz of ideal mixing between $V_8$ and $\mathcal{V}_1$. The departure from this situation is reviewed, using different models, in Ref. [28]. The amount of deviation from ideal mixing in the $\phi$–$\omega$ system has been estimated [7] to influence, in an analysis of the present kind, the determination of the magnitude of the OZI violation at the $\sim$5% level. This should be compared with the expected $\sim$40% departure from unity [7] of the parameter $\nu$ in Eq. (2). In view of this, the relations given in Eqs. (3) and (4) will be considered adequate for the present analysis.

[1]The scalar FFs of the pion in Ref. [7] require a minor correction in the values at $s = 0$. The authors thank J. Bijnens and J. A. Oller for their assistance in pinpointing this. The effect on the numerics of Ref. [7] is negligible.

The scalar sources $S_\phi$ and $S_\omega$ may, in terms of a quark model description, be expressed as $S_\phi = \bar{s}s$ and $S_\omega = \bar{n}n \equiv (\bar{u}u + \bar{d}d)/\sqrt{2}$. By means of these relations and Eqs. (3) and (4), the Lagrangian of Eq. (2) may be written in the form

$$\mathcal{L} = \Psi_\mu \phi^\mu C_\phi(\nu)[\bar{s}s + \lambda_\phi(\nu)\bar{n}n] + \Psi_\mu \omega^\mu C_\omega(\nu)[\bar{s}s + \lambda_\omega(\nu)\bar{n}n], \tag{5}$$

where the coupling constant $g$ is taken, as further elaborated in Sec. II B, to be absorbed into $C_\phi$ and $C_\omega$. These and the $\lambda_i$ in Eq. (5) are given in terms of the parameter $\nu$ according to

$$\lambda_\phi = \frac{\sqrt{2}(\nu - 1)}{2 + \nu}, \qquad C_\phi = \frac{2 + \nu}{3}, \tag{6}$$

$$\lambda_\omega = \frac{1 + 2\nu}{\sqrt{2}(\nu - 1)}, \qquad C_\omega = \frac{\sqrt{2}(\nu - 1)}{3}, \tag{7}$$

which shows that the parameters for the $\omega$ decay operator can be expressed in terms of those which control the $\phi$ decay. The explicit relations are given by

$$C_\omega = \lambda_\phi C_\phi, \qquad \lambda_\omega = \frac{\lambda_\phi + \sqrt{2}}{\sqrt{2}\lambda_\phi}. \tag{8}$$

From now on, the dependence of the $C_i$ and $\lambda_i$ on $\nu$ will be suppressed. The quantities to be determined from fits to the experimental dimeson spectra of Refs. [12–14] are taken to be $C_\phi$ and $\lambda_\phi$. It is worth noting that the limit $\lambda_\phi = 0$ corresponds to the value $\nu = 1$, and in that case the dimeson spectra for $\phi$ and $\omega$ decays are driven entirely by the strange scalar source $\bar{s}s$ and the nonstrange scalar source $\bar{n}n$, respectively.

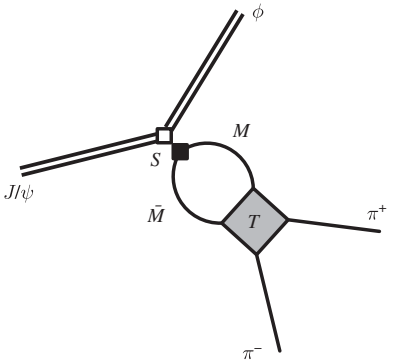


FIG. 2. Overview of the decay $J/\psi \to \phi\pi^+\pi^-$. The open square represents a vertex of the Lagrangian in Eq. (1), whereas the solid square denotes the scalar FF of the pseudoscalar meson pair $M\bar{M}$ to NLO in CHPT. The shaded square represents the $T$-matrix for meson-meson scattering, as calculated from the LO CHPT amplitudes via the Bethe-Salpeter equation. The interpolating field $S$ corresponds to the strange and nonstrange scalar sources $\bar{s}s$ and $\bar{n}n$, as described in the text.

From the Lagrangian in Eq. (5), the matrix elements for $\phi\pi^+\pi^-$ and $\phi K^+K^-$ decay of the $J/\psi$ are given by

$$\mathcal{M}_\phi^{\pi\pi} = \sqrt{\frac{2}{3}} C_\phi \langle 0|(\bar{s}s + \lambda_\phi \bar{n}n)|\pi\pi\rangle^*_{I=0}, \tag{9}$$

$$\mathcal{M}_\phi^{KK} = \sqrt{\frac{1}{2}} C_\phi \langle 0|(\bar{s}s + \lambda_\phi \bar{n}n)|K\bar{K}\rangle^*_{I=0}, \tag{10}$$

in terms of the $\pi\pi$ and $K\bar{K}$ states with $I = 0$, which are related to the physical $\pi^+\pi^-$ and $K^+K^-$ states by the Clebsch-Gordan (CG) coefficients in front of the above expressions. It should be noted that in Ref. [7], the CG-coefficient for $\pi^+\pi^-$ decay was incorrectly written as $\sqrt{4/3}$. The full transition amplitudes also contain the polarization vectors of the $J/\psi$ and $\phi$ mesons, which have not been included in the above definitions. They introduce an additional, weakly energy dependent factor which is given explicitly in Sec. II B. The matrix elements for $\omega\pi^+\pi^-$ and $\omega K^+K^-$, may be obtained by replacement of the labels in Eqs. (9) and (10) according to $\phi \to \omega$. The matrix elements of the scalar sources are given in terms of the $I = 0$ scalar FFs which are discussed in Sec. II C.

### B. Decay rates and dimeson event distributions

The differential decay rate of a $J/\psi$ into a vector meson and a pair of pseudoscalar mesons is, for the case of $\phi\pi\pi$ decay, given by

$$\frac{d\Gamma}{dW_{\pi\pi}} = \frac{W_{\pi\pi}|\vec{p}_\phi||\vec{p}_\pi|}{4M^3_{J/\psi}(2\pi)^3} F_{\rm pol} |\mathcal{M}_\phi^{\pi\pi}|^2, \tag{11}$$

where $W_{\pi\pi} = \sqrt{s_{\pi\pi}}$. The decay rates for the other combinations of $\phi$ and $\omega$ mesons and $\pi\pi$, $K\bar{K}$ final states can be obtained by appropriate replacement of the indices in Eq. (11). The moduli of the $\phi$ and $\pi$ momenta in Eq. (11) are given by

$$|\vec{p}_\phi| = \sqrt{E_\phi^2 - m_\phi^2}, \qquad E_\phi = \frac{M^2_{J/\psi} - W^2_{\pi\pi} - m^2_\phi}{2W_{\pi\pi}}, \tag{12}$$

$$|\vec{p}_\pi| = \sqrt{E_\pi^2 - m_\pi^2}, \qquad E_\pi = W_{\pi\pi}/2, \tag{13}$$

in the rest frame of the $\pi\pi$ system. The factor $F_{\rm pol}$ in Eq. (11) depends on the dipion energy $W_{\pi\pi}$ and is generated by properly averaging and summing over the polarizations of the $J/\psi$ and $\phi$ mesons, respectively. It may be expressed as

$$F_{\rm pol} \equiv \frac{1}{3}\sum_{\rho,\rho'} \varepsilon_\mu(\rho)\varepsilon^\mu(\rho')\varepsilon^*_\nu(\rho)\varepsilon^{\nu*}(\rho') = \frac{2}{3}\left[1 + \frac{(M^2_{J/\psi} + M^2_\phi - W^2_{\pi\pi})^2}{8M^2_{J/\psi}M^2_\phi}\right]. \tag{14}$$

Again, it should be noted that the corresponding expressions for $F_{\rm pol}$ for the other decay channels considered can be obtained straightforwardly from Eq. (14) by the substitutions $\phi \to \omega$ and $\pi\pi \to K\bar{K}$.

The results for $J/\psi$ decay into a vector meson and a dimeson pair published by the BES collaboration are given in terms of event distributions as a function of the dimeson center-of-mass energy $W$. The relation between the differential event distribution and the decay rate given by Eq. (11) is defined to be

$$\frac{dN}{dW_{\pi\pi}} \sim \eta(W_{\pi\pi}) \frac{d\Gamma}{dW_{\pi\pi}}, \tag{15}$$

where the function $\eta(W)$ represents the detection efficiency, shown in Fig. 3, which also takes into account the effects of the various cuts imposed on the data in order to reduce the background to an acceptable level. It should be noted that the detection efficiencies $\eta$ cannot be neglected, since it is evident from Fig. 3 that a sizeable difference exists between the efficiencies for all four decays considered. Furthermore, the detection efficiencies exhibit significant nonlinear behavior.

The overall constant of proportionality in Eq. (15) is not relevant to the present analysis, since it may be absorbed in the definitions of $C_\phi$ and $C_\omega$, along with the coupling constant $g$ of Eq. (2) and a factor $\sqrt{2}B_0$ from the scalar FFs in Eq. (19). Thus, the quantities with $\sqrt{2}gB_0$ and the proportionality factor absorbed are denoted by $\tilde{C}_\phi$ and $\tilde{C}_\omega$. While $C_\phi$ and $gB_0$ are dimensionless, $\tilde{C}_\phi$ has dimension $[E^{-1/2}]$.

### C. Scalar form factors from CHPT

The nonstrange and strange scalar FFs of the pseudo-Goldstone bosons of CHPT are defined in terms of the $S$-wave states with $I = 0$,

$$|\pi\pi\rangle_{I=0} = \frac{1}{\sqrt{3}}|\pi^+\pi^-\rangle + \frac{1}{\sqrt{6}}|\pi^0\pi^0\rangle, \tag{16}$$

$$|K\bar{K}\rangle_{I=0} = \frac{1}{\sqrt{2}}|K^+K^-\rangle + \frac{1}{\sqrt{2}}|K^0\bar{K}^0\rangle, \tag{17}$$

$$|\eta\eta\rangle_{I=0} = \frac{1}{\sqrt{2}}|\eta\eta\rangle, \tag{18}$$

where $|\pi^+\pi^-\rangle$ denotes the symmetrized combination of $|\pi^+\pi^-\rangle$ and $|\pi^-\pi^+\rangle$. Following the conventions of Refs. [29–31], an extra factor of $1/\sqrt{2}$ has been included for the $I = 0$ states composed of members of the same isospin multiplet. This takes conveniently into account the fact that the pions behave as identical particles in the isospin basis. In terms of the above states, the scalar FFs

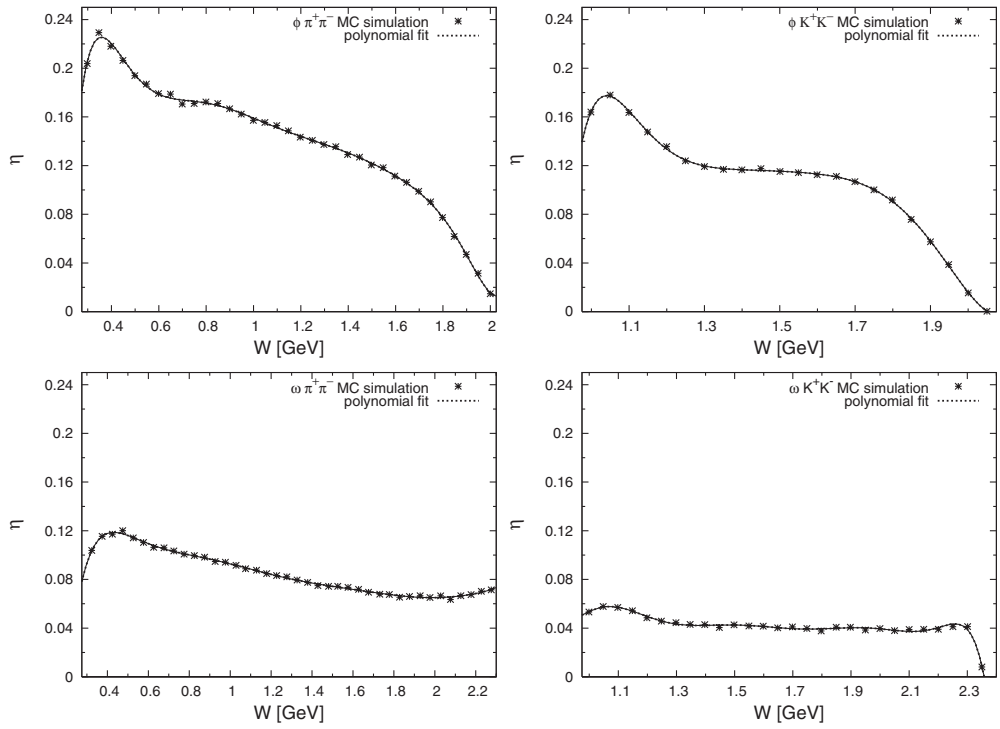


FIG. 3. Detection efficiency $\eta$ from BES Monte Carlo simulations for $J/\psi \to \phi\pi^+\pi^-$, $J/\psi \to \phi K^+K^-$, $J/\psi \to \omega\pi^+\pi^-$ and $J/\psi \to \omega K^+K^-$, along with fitted polynomial approximations for each case. The estimated detection efficiencies take into account the characteristics of the BES detector as well as the different cuts applied in the data analysis. The BES data published in Refs. [12–14] are uncorrected for efficiency, and for that purpose the efficiency functions $\eta$ have been included in Eq. (15).

for the $\pi$, $K$ and $\eta$ mesons are defined as

$$\sqrt{2}B_0\Gamma_1^n(s) = \langle 0|\bar{n}n|\pi\pi\rangle_{I=0},$$
$$\sqrt{2}B_0\Gamma_2^n(s) = \langle 0|\bar{n}n|K\bar{K}\rangle_{I=0}, \quad (19)$$
$$\sqrt{2}B_0\Gamma_3^n(s) = \langle 0|\bar{n}n|\eta\eta\rangle_{I=0},$$

where the notation ($\pi = 1$, $K = 2$, $\eta = 3$) has been introduced for simplicity. The expressions for the strange scalar FFs may be obtained by the substitutions $\Gamma_i^n \to \Gamma_i^s$ and $\bar{n}n \to \bar{s}s$. As discussed above, the expressions given in Ref. [7] are updated here with minor corrections to $\Gamma_1^n$ and $\Gamma_1^s$. With these definitions, the scalar FFs may be expressed in terms of the meson loop function $J_{ii}^r$ [17] and the tadpole factor $\mu_i$, given in Eqs. (31) and (33) respectively. The expressions so obtained up to NLO in CHPT are, in agreement with Refs. [17,32,33],

$$\Gamma_1^n(s) = \sqrt{\frac{3}{2}}\Big[1 + \mu_\pi - \frac{\mu_\eta}{3} + \frac{16m_\pi^2}{f^2}(2L_8^r - L_5^r) + 8(2L_6^r - L_4^r)\frac{2m_K^2 + 3m_\pi^2}{f^2} + \frac{8s}{f^2}L_4^r + \frac{4s}{f^2}L_5^r + \left(\frac{2s - m_\pi^2}{2f^2}\right)J_{\pi\pi}^r(s) + \frac{s}{4f^2}J_{KK}^r(s) + \frac{m_\pi^2}{18f^2}J_{\eta\eta}^r(s)\Big], \quad (20)$$

$$\Gamma_1^s(s) = \frac{\sqrt{3}}{2}\Big[\frac{16m_\pi^2}{f^2}(2L_6^r - L_4^r) + \frac{8s}{f^2}L_4^r + \frac{s}{2f^2}J_{KK}^r(s) + \frac{2}{9}\frac{m_\pi^2}{f^2}J_{\eta\eta}^r(s)\Big], \quad (21)$$

for the pion, and

$$\Gamma_2^n(s) = \frac{1}{\sqrt{2}}\Big[1 + \frac{8L_4^r}{f^2}(2s - m_\pi^2 - 6m_K^2) + \frac{4L_5^r}{f^2}(s - 4m_K^2) + \frac{16L_6^r}{f^2}(6m_K^2 + m_\pi^2) + \frac{32L_8^r}{f^2}m_K^2 + \frac{2}{3}\mu_\eta + \left(\frac{9s - 8m_K^2}{36f^2}\right)J_{\eta\eta}^r(s) + \frac{3s}{4f^2}J_{KK}^r(s) + \frac{3s}{4f^2}J_{\pi\pi}^r(s)\Big], \quad (22)$$

$$\Gamma_2^s(s) = 1 + \frac{8L_4^r}{f^2}(s - m_\pi^2 - 4m_K^2) + \frac{4L_5^r}{f^2}(s - 4m_K^2) + \frac{16L_6^r}{f^2}(4m_K^2 + m_\pi^2) + \frac{32L_8^r}{f^2}m_K^2 + \frac{2}{3}\mu_\eta + \left(\frac{9s - 8m_K^2}{18f^2}\right)J_{\eta\eta}^r(s) + \frac{3s}{4f^2}J_{KK}^r(s), \quad (23)$$

for the kaon. Finally, for the $\eta$ one finds

$$\Gamma_3^n(s) = \frac{1}{2\sqrt{3}}\Big[1 + \frac{24L_4^r}{f^2}\Big(s + \frac{1}{3}m_\pi^2 - \frac{10}{3}m_K^2\Big) + \frac{4L_5^r}{f^2}\Big(s + \frac{4}{3}m_\pi^2 - \frac{16}{3}m_K^2\Big) + \frac{16L_6^r}{f^2}(10m_K^2 - m_\pi^2) + \frac{128L_7^r}{f^2}(m_\pi^2 - m_K^2) + \frac{32L_8^r}{f^2}m_\pi^2 - \frac{\mu_\eta}{3} + 4\mu_K - 3\mu_\pi + \left(\frac{16m_K^2 - 7m_\pi^2}{18f^2}\right)J_{\eta\eta}^r(s) + \left(\frac{9s - 8m_K^2}{4f^2}\right)J_{KK}^r(s) + \frac{3}{2}\frac{m_\pi^2}{f^2}J_{\pi\pi}^r(s)\Big], \quad (24)$$

$$\Gamma_3^s(s) = \frac{2}{3}\Big[1 + \frac{6L_4^r}{f^2}\Big(s - \frac{2}{3}m_\pi^2 - \frac{16}{3}m_K^2\Big) + \frac{4L_5^r}{f^2}\Big(s + \frac{4}{3}m_\pi^2 - \frac{16}{3}m_K^2\Big) + \frac{8L_6^r}{f^2}(8m_K^2 + m_\pi^2) + \frac{64L_7^r}{f^2} \times (m_K^2 - m_\pi^2) + \frac{32L_8^r}{f^2}(2m_K^2 - m_\pi^2) - \frac{4}{3}\mu_\eta + 2\mu_K + \left(\frac{16m_K^2 - 7m_\pi^2}{18f^2}\right)J_{\eta\eta}^r(s) + \left(\frac{9s - 8m_K^2}{8f^2}\right)J_{KK}^r(s)\Big]. \quad (25)$$

### D. Matching of FSI to NLO CHPT

The constraints imposed by unitarity on the pion and kaon scalar FFs, the inclusion of the FSI via resummation in terms of the Bethe-Salpeter (BS) equation, the channel coupling between the $\pi\pi$ and $K\bar{K}$ systems, and the matching of the scalar FFs to the NLO CHPT expressions have all been elaborated in great detail in Refs. [7,15], and will thus be only briefly touched upon here. Within that framework, consideration of the unitarity constraints yields a scalar FF in terms of the algebraic coupled-channel equation

$$\Gamma(s) = [I + K(s)g(s)]^{-1}R(s) = [I - K(s)g(s)]R(s) + \mathcal{O}(p^6), \quad (26)$$

where in the second line, the equation has been expanded up to NLO, the NNLO contribution defined as being of $\mathcal{O}(p^6)$ in the chiral expansion. This expansion is instructive since it allows for the $J_{ii}^r$ integrals from the NLO scalar FF expressions to be absorbed into the above equation. Here $K(s)$ denotes the kernel of $S$-wave projected $I = 0$ meson-meson scattering amplitudes from the leading order chiral Lagrangian. Using the notation defined in Sec. II C, they are given by

$$K_{11} = \frac{2s - m_\pi^2}{2f^2}, \qquad K_{12} = K_{21} = \frac{\sqrt{3}s}{4f^2}, \qquad K_{22} = \frac{3s}{4f^2}, \tag{27}$$

where the constant $f$ is taken to equal the pion decay constant $f_\pi$, with the convention $f_\pi = 0.0924$ GeV. The components given above are sufficient for the two-channel formalism of Ref. [7] used in this paper, where only the FSI in the $\pi\pi$ and $K\bar{K}$ channels is considered. The chiral logarithms associated with the $\eta\eta$ channel can thus not be reproduced by Eq. (26) and are therefore removed from the chiral expressions given in Sec. II C, while the contribution of that channel to the values of the form factors at $s = 0$ is retained. For completeness, it should be noted that if the $\eta\eta$ channel is also included, then the matrix $K(s)$ should be augmented by the elements

$$K_{13} = K_{31} = \frac{m_\pi^2}{2\sqrt{3}f^2}, \qquad K_{33} = \frac{16m_K^2 - 7m_\pi^2}{18f^2}, \qquad K_{23} = K_{32} = \frac{9s - 8m_K^2}{12f^2}. \tag{28}$$

The elements of the diagonal matrix $g_i(s)$ in Eq. (26) are given by the cutoff-regularized loop integral

$$g_i(s) = \frac{1}{16\pi^2}\left\{\sigma_i(s)\log\left(\frac{\sigma_i(s)\sqrt{1 + \frac{m_i^2}{q_{\max}^2}} + 1}{\sigma_i(s)\sqrt{1 + \frac{m_i^2}{q_{\max}^2}} - 1}\right) - 2\log\left[\frac{q_{\max}}{m_i}\left(1 + \sqrt{1 + \frac{m_i^2}{q_{\max}^2}}\right)\right]\right\}, \tag{29}$$

where

$$\sigma_i(s) = \sqrt{1 - \frac{4m_i^2}{s}}, \tag{30}$$

and $q_{\max}$ denotes a three-momentum cutoff, which has to be treated as an *a priori* unknown model parameter, which is however expected to be of the order of $\sim$1 GeV. Since the above expressions are calculated in a cutoff-regularization scheme, it is useful to note that within the modified $\overline{MS}$ subtraction scheme commonly employed in CHPT, the meson loop function $g_i(s)$ is given by

$$J_{ii}^r(s) \equiv \frac{1}{16\pi^2}\left[1 - \log\left(\frac{m_i^2}{\mu^2}\right) - \sigma_i(s)\log\left(\frac{\sigma_i(s) + 1}{\sigma_i(s) - 1}\right)\right] = -g_i(s), \tag{31}$$

for which it has been shown in App. 2 of Ref. [29] that an optimal matching between the two renormalization schemes requires that

$$\mu = \frac{2q_{\max}}{\sqrt{e}}, \tag{32}$$

in which case the differences between the two forms are of $\mathcal{O}(m_i^2/q_{\max}^2)$. Furthermore, the expressions for the logarithms $\mu_i$ generated by the chiral tadpoles in the NLO scalar FFs are given by

$$\mu_i = \frac{m_i^2}{32\pi^2 f^2}\log\left(\frac{m_i^2}{\mu^2}\right). \tag{33}$$

As demonstrated in Ref. [7], the quantity $R(s)$ in Eq. (26) is a vector of functions free of any cuts or singularities, since the right-hand or unitarity cut has been removed by construction. The information provided by CHPT can then be built into the formalism by fixing $R(s)$ to the NLO CHPT expressions for the scalar FFs. Consideration of Eq. (26) yields the defining relations

$$\Gamma_i^n(s) = R_i^n(s) - \sum_{j=1}^{2} K_{ij}(s)g_j(s)R_j^n(s) + \mathcal{O}(p^6), \tag{34}$$

where it is understood that only contributions up to $\mathcal{O}(p^4)$ are to be retained in the product $KgR$. The analogous expressions for the vectors $R_i^s(s)$ associated with the strange scalar FFs $\Gamma_i^s(s)$ can be obtained from the above relations by the substitutions $\Gamma_i^n \to \Gamma_i^s$ and $R_i^n \to R_i^s$. The above procedure is equivalent to the intuitive result obtained by dropping, in the expressions for the $\Gamma_i$, all occurrences of the loop integrals $J_{\pi\pi}^r$ and $J_{KK}^r$, and keeping only the parts of the $J_{\eta\eta}^r$ which do not depend on $s$. Nevertheless, the explicit evaluation of Eq. (34) provides a useful check on the consistency of the normalization used for the NLO scalar FFs and the LO meson-meson interaction kernel $K$. It should also be noted that the expressions for $R_1^n$ and $R_1^s$ correspond to the corrected scalar FFs, as explained in the beginning of Sec. II. The expressions for the $R^i$ so obtained are

$$R_1^n(s) = \sqrt{\frac{3}{2}}\left\{1 + \mu_\pi - \frac{\mu_\eta}{3} + \frac{16m_\pi^2}{f^2}(2L_8^r - L_5^r) + 8(2L_6^r - L_4^r)\frac{2m_K^2 + 3m_\pi^2}{f^2} + \frac{8s}{f^2}L_4^r + \frac{4s}{f^2}L_5^r - \frac{m_\pi^2}{288\pi^2 f^2}\left[1 + \log\left(\frac{m_\eta^2}{\mu^2}\right)\right]\right\}, \tag{35}$$

$$R_1^s(s) = \frac{\sqrt{3}}{2}\left\{\frac{16m_\pi^2}{f^2}(2L_6^r - L_4^r) + \frac{8s}{f^2}L_4^r - \frac{m_\pi^2}{72\pi^2 f^2}\left[1 + \log\left(\frac{m_\eta^2}{\mu^2}\right)\right]\right\}, \tag{36}$$

for the pion, and for the kaon one finds

$$R_2^n(s) = \frac{1}{\sqrt{2}}\Big\{1 + \frac{8L_4^r}{f^2}(2s - 6m_K^2 - m_\pi^2) + \frac{4L_5^r}{f^2}(s - 4m_K^2) + \frac{16L_6^r}{f^2}(6m_K^2 + m_\pi^2) + \frac{32L_8^r}{f^2}m_K^2 + \frac{2}{3}\mu_\eta + \frac{m_K^2}{72\pi^2 f^2}\Big[1 + \log\Big(\frac{m_\eta^2}{\mu^2}\Big)\Big]\Big\}, \quad (37)$$

$$R_2^s(s) = 1 + \frac{8L_4^r}{f^2}(s - 4m_K^2 - m_\pi^2) + \frac{4L_5^r}{f^2}(s - 4m_K^2) + \frac{16L_6^r}{f^2}(4m_K^2 + m_\pi^2) + \frac{32L_8^r}{f^2}m_K^2 + \frac{2}{3}\mu_\eta + \frac{m_K^2}{36\pi^2 f^2}\Big[1 + \log\Big(\frac{m_\eta^2}{\mu^2}\Big)\Big]. \quad (38)$$

The expressions for the $R_i^n$ and $R_i^s$ are valid when only the $\pi\pi$ and $K\bar{K}$ channels are considered in the FSI. On the other hand, if the full three-channel interaction kernel of Eq. (27) is used, then the above equations should be modified such that the terms in square brackets are dropped. With respect to the omission of the $\eta\eta$ channel, it was noted in Ref. [23] that reproduction of the data on the inelastic $\pi\pi \to K\bar{K}$ cross section requires the addition of a preexisting contribution to the $f_0(980)$ if the $\eta\eta$ channel is included. On the other hand, no such contribution was found to be necessary if the $\eta\eta$ channel is dropped. Furthermore, the effect of this channel is known [23] to be very small for energies less than $\sim$0.8 GeV.

It should be stressed here, with respect to the above mentioned issues, that the main concern in the present analysis is the use of a meson-meson interaction kernel which is known to give a realistic description of the $\pi\pi$ phase shift close to the $K\bar{K}$ threshold. Since none of the adjustable model parameters have any influence on the behavior of the $\pi\pi$ phase shift, any model which has the proper chiral behavior for low energies and faithfully reproduces the $f_0(980)$ should therefore give similar results. In view of this, the inclusion or omission of the $\eta\eta$ channel, or the question of a preexisting contribution to the $f_0(980)$ resonance, are issues of secondary importance. Nevertheless, the uncertainties introduced by these issues into the determination of the $L_i^r$ are discussed in Sec. III. Finally, it should be noted that in order to minimize the dependence on $m_\eta$, the Gell-Mann-Okubo (GO) relation has been applied throughout in the polynomial terms of the $\Gamma_i$ and the $R_i$.

## III. FITS TO BES DATA

The event distributions given by Eq. (15) can be simultaneously fitted to the dimeson spectra in the $\phi\pi^+\pi^-$, $\omega\pi^+\pi^-$ and $\phi K^+K^-$ channels. The parameters to be determined via a $\chi^2$ fit are the LECs $L_4^r$, $L_5^r$, $L_6^r$ and $L_8^r$ which influence the scalar FFs, as well as the model parameters $\tilde{C}_\phi$ and $\lambda_\phi$. Because of the accuracy of the BES data [12–14], all of the model parameters can be well constrained, which is especially true for $L_4^r$ and $\lambda_\phi$, while the sensitivity of the fit to $L_5^r$ and $L_8^r$ turns out to be somewhat less. Once all the model parameters are determined by a fit to the three decay channels mentioned above, the event distribution in the remaining $\omega K^+K^-$ channel in essentially fixed. This channel is thus not included in the fit and is treated instead as a prediction. To a large extent, this also turns out to be true for the shape of the fitted $\omega\pi^+\pi^-$ distribution.

In spite of the above mentioned positive issues, the fitting of the predicted event distribution $dN/dW$ to the $S$-wave contribution from the PWA of the BES collaboration is complicated by several issues: Firstly, the detection efficiencies, determined by BES via Monte Carlo simulation and shown in Fig. 3, are different for each decay channel, and furthermore vary appreciably over the range of dimeson energies considered. Secondly, the $S$-wave contribution in the BES PWA cannot be considered as strict experimental information, since it is inevitably biased to some extent by the parametrizations chosen there for the $\sigma$ pole. Thirdly, an unambiguous fit requires a highly precise description of the $f_0(980)$ resonance generated by the FSI, which to a large extent cannot be adjusted in the present model. All of these issues, as well as the fitted parameter values and the associated error analysis are elaborated in detail below.

### A. Definitions

In order for the fit results to be well reproducible, the various constant parameters which enter the expressions for the decay amplitudes should be accurately defined. These parameters include the masses of the light pseudoscalar mesons, for which the current experimental values [34] have been used. These are $m_\pi = 0.13957$ GeV, $m_K = 0.49368$ GeV and $m_\eta = 0.5478$ GeV, while the value $f_\pi = 0.0924$ GeV has been adopted for the pion decay constant. The physical masses of the charged pions and kaons have been used in order for the $\pi^+\pi^-$ and $K^+K^-$ thresholds to coincide with the physical ones. Also, the physical $\eta$ meson mass has been used rather than the one given by the GO relation. The $\eta$ meson mass appears in relatively few places in the expressions, and checks on the fits have indicated that replacement of the physical $\eta$ mass with that given by the GO relation has a minimal effect. Further parameters are the masses of the vector mesons $\rho$, $\omega$, $\phi$ and $J/\psi$. The $\rho$ mass is used in the evolution of the $L_i^r$, and has been taken as $m_\rho = 0.776$ GeV. The other vector meson masses appear in various phase-space factors, and have been given the values $m_\omega = 0.783$ GeV, $m_\phi = 1.020$ GeV and $m_{J/\psi} = 3.097$ GeV [34].

It is not *a priori* obvious how the individual deviations, required for the $\chi^2$ fit, are to be treated for the BES data. The individual deviations for each bin $\sigma_i$, are given by the BES collaboration as the square root of the number of

events $\sqrt{N_i}$. These numbers represent the statistical errors of the raw data, uncorrected for detection efficiency and background. Furthermore, what is fitted in the present analysis is not the total signal detected by the BES experiment, but rather the $S$-wave contribution from the accompanying PWA. In view of these considerations, the deviations for each bin used in the fitting procedure have been taken to be of the form

$$\Delta_i \equiv \sqrt{N_i} w_i, \tag{39}$$

where the $w_i$ represent weighting factors which have been chosen in a physically motivated way. In principle, individual $w_i$ could be introduced in all the decay channels studied and would then represent a ''quality factor'' for each bin. In practice, to avoid excessive fine-tuning of the fit, a constant value for $w_i$ has been applied for each decay channel, according to the following principles: Since the $S$-wave contribution in the $\omega\pi^+\pi^-$ spectrum is likely to have the largest uncertainty, a value of $w_i = 3$ has been adopted for that decay channel, whereas the values of $w_i$ for the $\phi\pi^+\pi^-$ and $\phi K^+K^-$ distributions have been defined to be between 0 and 1. The choice of such a large value of $w_i$ for $\omega\pi^+\pi^-$ means that the shape of the $\pi^+\pi^-$ spectrum is constrained by the $\phi\pi^+\pi^-$ and $\phi K^+K^-$ distributions, and may therefore be considered as a prediction of the present analysis. On the other hand, the relative magnitude of the $\phi\pi^+\pi^-$ and $\omega\pi^+\pi^-$ spectra provides an important piece of experimental input, without which all parameters in the fit cannot be constrained. Checks have been performed to verify that the choice of $w_i = 3$ for $\omega\pi^+\pi^-$ does not introduce unphysical skewing of the fit, and it was found that a further increase in $w_i$ for $\omega\pi^+\pi^-$ has a negligible effect on the fit results. The values for $w_i$ used for the other two channels are $w_i = 1$ for $\phi\pi^+\pi^-$ and $w_i = 0.1$ for $\phi K^+K^-$ in ''Fit I'' and vice versa for ''Fit II''. Again, the fit results have been checked for stability with respect to these choices.

The predicted number of events $N_i$ in each bin is fitted to the total number of $S$-wave events determined by the BES PWA. To this end, the definition

$$\bar{N}(W) \equiv \left(\frac{dN}{dW}\right)\Delta W, \tag{40}$$

has been implemented, where the differential event distribution $dN/dW$ is given by Eq. (15), and $\Delta W$ denotes the binsize chosen by BES for the PWA, given as 25 MeV for $\omega$ final states and 30 MeV for $\phi$ final states [12–14]. It should be reemphasized that all effects due to detection efficiencies are included in $dN/dW$ as defined in Eq. (15). The number of events $N_i$ per bin are then calculated by averaging Eq. (40) over the energy range $[W_1^i, W_2^i]$ spanned by the bin, giving

$$N_i = \frac{1}{\Delta W}\int_{W_1^i}^{W_2^i} \bar{N}(W) dW, \tag{41}$$

where the explicit dependence on the binsize $\Delta W$ cancels. The advantage of the function $\bar{N}(W)$ is that it can be conveniently compared with the experimental data, regardless of the binsize chosen for a particular decay channel.

Finally, the $L_i^r$ determined in the fit are always quoted at the scale $\mu = m_\rho$. The fit function itself depends on the $L_i^r$ at the scale given by Eq. (32) in terms of the cutoff parameter $q_{\max}$ of the FSI, which gives the $L_i^r$ at a scale of $\mu \sim 1.2 q_{\max}$. For calculational purposes, the $L_i^r$ are evolved to this scale.

### B. Error analysis

All fits in this work are performed by minimizing the $\chi^2$ with respect to the $S$-wave event distributions reported by the BES PWA [12–14] for $\phi\pi^+\pi^-$, $\omega\pi^+\pi^-$ and $\phi K^+K^-$. The only parameter left fixed in all of the fits is the momentum cutoff $q_{\max}$, which is constrained by the requirement that the $f_0(980)$ resonance generated by the FSI should be well centered on the corresponding peak in the experimental $\phi\pi^+\pi^-$ spectrum. A rather broad $\chi^2$ minimum is found around a cutoff of $\sim$0.9 GeV, and in order to avoid unnecessary fine-tuning, that value is taken as the central value to be used in all fits. To estimate the uncertainty associated with the choice of $q_{\max}$, a range of 50 MeV, between $q_{\max} = 0.875$ GeV and $q_{\max} = 0.925$ GeV, has been considered. Larger or smaller values produce an $f_0(980)$ peak which is no longer well centered on the experimental one in $\phi\pi^+\pi^-$. In order to illustrate the dependence on the choice of cutoff $q_{\max}$, fits for a fixed cutoff, each corresponding to the values quoted above, have been given in Table I as ''Fit Ia–Ic''.

The statistical errors of the BES data [12–14] are small and have little bearing on the actual sources of uncertainties of the fitted parameters. The main sources of error accounted for in the present analysis are as follows: Firstly, the $\sigma$ amplitude used in the PWA for $\omega\pi^+\pi^-$ published by BES [13] did not take into account channel-coupling effects, which leads to a considerable uncertainty in the $S$-wave contribution close to the $K\bar{K}$ threshold. In view of this, the $\omega\pi^+\pi^-$ data is only fitted up to bin 30 and the uncertainty on the parameter values introduced by this arbitrary choice is estimated via fits up to bins 29 and 31. It is found that the effect of this is rather small for most parameters, and all of the fits contain a sharp characteristic cutoff in the $S$-wave $\pi^+\pi^-$ distribution close to the $K\bar{K}$ threshold. Secondly, the precise magnitude and shape of the $S$-wave contribution to the conspicuous low-energy enhancement, or $\sigma$ peak in the $\omega\pi^+\pi^-$ data has to be considered as somewhat uncertain, as the BES PWA models the $\sigma$ contribution in terms of different functional forms related to a relativistic Breit-Wigner description. Such approaches are known to suffer from consistency problems with respect to the data on $\pi\pi$ phase shifts, and indeed only one of the BES fits takes those data simultaneously

TABLE I. Parameter values obtained from a simultaneous fit to the BES results [12–14] for $J/\psi \to \phi\pi^+\pi^-$, $J/\psi \to \phi K^+K^-$ and $J/\psi \to \omega\pi^+\pi^-$. All values of the $L_i^r$ are quoted at the scale $\mu = m_\rho$. The meson masses and other input parameters are given in Sec. III A, and the uncertainties of the parameters correspond to the error analysis described in Sec. III B. Fixed parameters not determined by the fits are given in parentheses. The fits of type I optimize agreement for $J/\psi \to \phi K^+K^-$, whereas type II fits do so for $J/\psi \to \phi\pi^+\pi^-$. Fits III and IV are similar to "Fit I" in the weighting of the input data. Note that "Fit I" represents the main result of this study, as elaborated in Sec. III. The dimeson spectra which correspond to the main fits (I and II) are shown in Fig. 4, and the corresponding sets of scalar FFs in Figs. 5 and 6.

| Fit | $L_4^r$ $[10^{-3}]$ | $L_5^r$ $[10^{-3}]$ | $L_6^r$ $[10^{-3}]$ | $L_8^r$ $[10^{-3}]$ | $\tilde{C}_\phi$ $[\mathrm{keV}^{-1/2}]$ | $\lambda_\phi$ | $q_{\max}$ [GeV] | $\langle r^2\rangle_s^\pi$ [fm$^2$] |
|---|---|---|---|---|---|---|---|---|
| I | $0.84^{+0.06}_{-0.05}$ | $0.45^{+0.08}_{-0.09}$ | $0.03^{+0.16}_{-0.13}$ | $0.33^{+0.14}_{-0.17}$ | $42.1^{+5.0}_{-5.0}$ | $0.132^{+0.018}_{-0.015}$ | $(0.90 \pm 0.025)$ | 0.657 |
| Ia | $0.817^{+0.048}_{-0.029}$ | $0.384^{+0.009}_{-0.021}$ | $-0.025^{+0.110}_{-0.079}$ | $0.328^{+0.133}_{-0.172}$ | $45.27^{+1.82}_{-3.07}$ | $0.133^{+0.017}_{-0.016}$ | (0.875) | 0.652 |
| Ib | $0.840^{+0.043}_{-0.023}$ | $0.450^{+0.006}_{-0.018}$ | $0.028^{+0.107}_{-0.075}$ | $0.325^{+0.129}_{-0.168}$ | $42.08^{+1.24}_{-2.49}$ | $0.132^{+0.016}_{-0.015}$ | (0.9) | 0.657 |
| Ic | $0.858^{+0.037}_{-0.022}$ | $0.520^{+0.006}_{-0.015}$ | $0.081^{+0.104}_{-0.078}$ | $0.323^{+0.134}_{-0.166}$ | $39.15^{+1.09}_{-2.03}$ | $0.131^{+0.016}_{-0.015}$ | (0.925) | 0.663 |
| II | $0.95^{+0.08}_{-0.03}$ | $0.25^{+0.24}_{-0.29}$ | $0.06^{+0.13}_{-0.08}$ | $0.18^{+0.21}_{-0.25}$ | $44.7^{+1.2}_{-4.4}$ | $0.104^{+0.025}_{-0.023}$ | $(0.90 \pm 0.025)$ | 0.659 |
| III | $0.94^{+0.05}_{-0.04}$ | $0.40^{+0.10}_{-0.12}$ | (0.20) | $0.12^{+0.11}_{-0.11}$ | $35.1^{+2.5}_{-2.6}$ | $0.123^{+0.015}_{-0.013}$ | $(0.90 \pm 0.025)$ | 0.670 |
| IV | (0.70) | $0.55^{+0.12}_{-0.10}$ | $-0.15^{+0.11}_{-0.07}$ | $0.55^{+0.13}_{-0.14}$ | $50.9^{+3.8}_{-6.4}$ | $0.162^{+0.024}_{-0.017}$ | $(0.90 \pm 0.025)$ | 0.634 |

into account. The $S$-wave contribution, as determined by the BES PWA constitutes about 60% of the total signal in the $\sigma$ peak of the $\omega\pi^+\pi^-$ spectrum. The fact that the properties of the $\sigma$ peak are strongly influenced by interference with rescattering effects in the $\omega\pi$ system has also been demonstrated in Ref. [8], where a sequential decay mechanism with intermediate vector and axial-vector mesons, e.g. $J/\psi \to b_1(1235)\pi \to \omega\pi\pi$ was investigated.

The situation in the BES PWA is similar, as most of the remaining events at the $\sigma$ peak are due to the interference of the $\sigma$ amplitude with the prominent $b_1(1235)$ and $\rho(1450)$ resonances in the $\omega\pi$ system. At higher energies, the left wing of the strong $D$-wave $f_2(1270)$ resonance also contributes significantly. The situation for the $\phi\pi^+\pi^-$ spectrum is much more straightforward since the $S$-wave contribution completely dominates the data up to the $K\bar{K}$ threshold, and also because of the much weaker interaction in the $\phi\pi$ system. The advantage of using the BES PWA is that the direct $S$-wave contribution to the $\sigma$ peak has been disentangled from the $b_1(1235)$ and $\rho(1450)$ contributions, such that a direct fit to the $S$-wave spectrum is possible without consideration of strong rescattering effects in the $\omega\pi$ system, which would introduce further uncertainties due to the modeling of such effects. The downside is that such uncertainties are included instead in the determination of the $S$-wave amplitude in the PWA.

In view of the above-mentioned issues, a conservative 10% uncertainty in the size of the $S$-wave contribution has been adopted for the $\omega\pi^+\pi^-$ spectrum to estimate the errors on the fitted parameter values. Moreover, as described in Sec. III A, the $\omega\pi^+\pi^-$ data has been given a rather low weight factor, and thus the shapes of the fitted spectra are essentially dictated by the $\phi\pi^+\pi^-$ and $\phi K^+K^-$ channels. Nevertheless, inclusion of the $\omega\pi^+\pi^-$ data in the fits is essential in order to provide information on the relative intensities of the $\phi\pi^+\pi^-$ and $\omega\pi^+\pi^-$ channels. Without that information, the model parameter $\tilde{C}_\phi$ cannot be properly constrained since the present BES data [12–14] are unnormalized, which was also the case in Ref. [7].

### C. Fit results for $\phi\pi^+\pi^-$ and $\phi K^+K^-$

The experimental dipion spectrum for $J/\psi \to \phi\pi^+\pi^-$ is dominated by the conspicuous $S$-wave $f_0(980)$ resonance, such that an accurate description of that state is necessary in order for a reasonable fit to be attained. In the present description, the $f_0(980)$ is dynamically generated and its appearance is a consequence of the channel coupling to $K\bar{K}$. However, since the FSI model depends on only one parameter, namely, the momentum cutoff $q_{\max}$, the possibilities of optimizing the width of that state are severely restricted. It is thus fortunate that the present considerations give a reasonable description of the $f_0(980)$, with the possible objection of that state being slightly too narrow. This generates an ambiguity which is reflected in the fact that two different fits, shown as "Fit I" and "Fit II" in Fig. 4, may be achieved depending on whether the $\phi\pi^+\pi^-$ or the $\phi K^+K^-$ spectrum is optimized.

As in the present case for "Fit II", agreement was optimized for $\phi\pi^+\pi^-$ in Ref. [7], which resulted in a noticeable underprediction of the $\phi K^+K^-$ spectrum. As explained in Sec. III A, "Fit I" was defined by forcing agreement with the $\phi K^+K^-$ spectrum, which may be accomplished at the small price of a moderate overprediction in the $\phi\pi^+\pi^-$ spectrum, which amounts to a factor $\sim$2 at the bin centered on the $f_0(980)$ peak. A comparison of the fitted parameter values given in Table I suggests that the ones corresponding to "Fit I" are more realistic. Further comparison of the two fits has also revealed that "Fit I" is more stable against variations in the input. It is thus concluded that "Fit I" is preferable and that the modest overprediction at the $f_0(980)$ resonance in the $\phi\pi^+\pi^-$ spectrum is due to the limitations of the FSI model employed in this paper. It should be emphasized that this discrepancy is small enough to go unnoticed in a

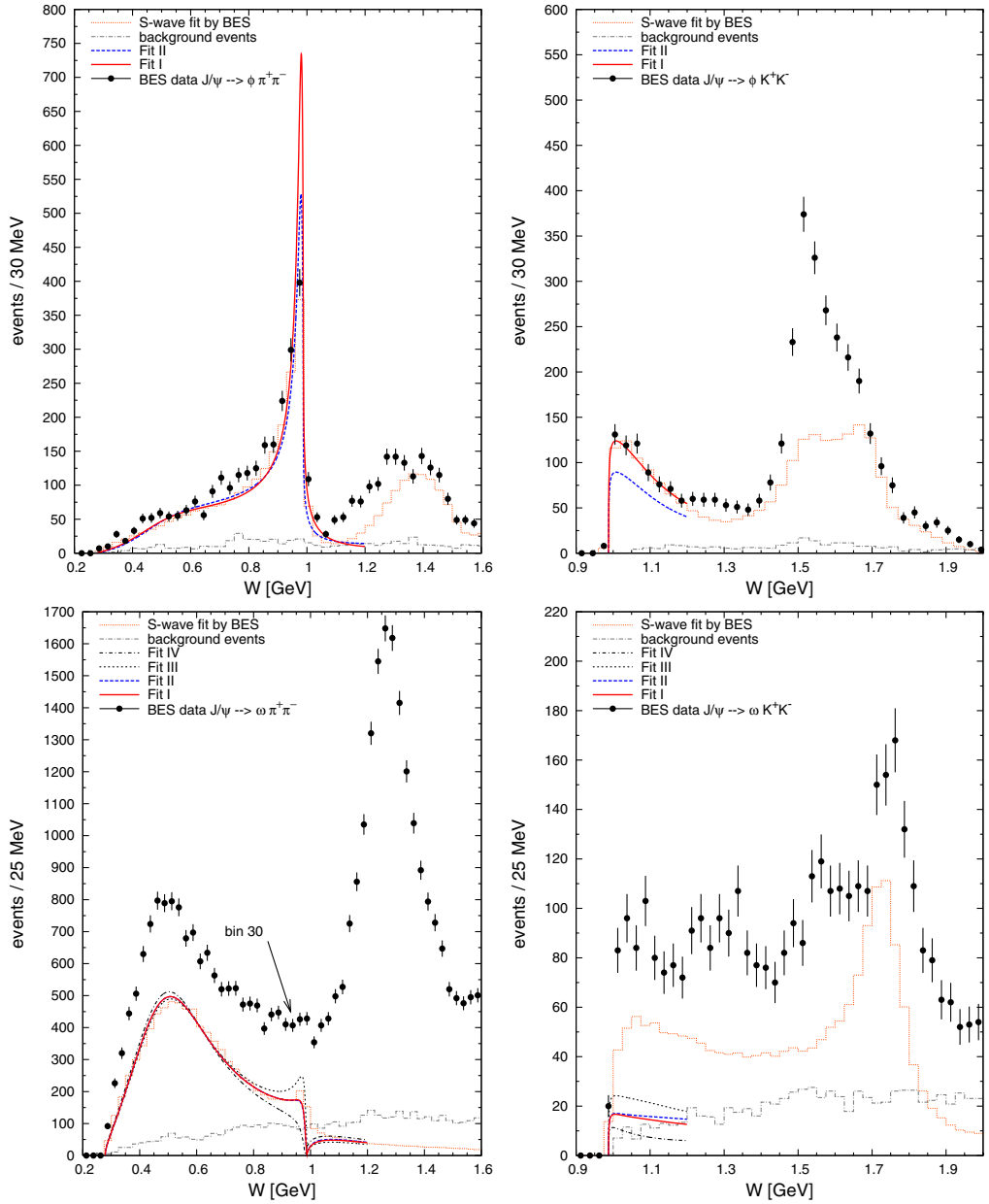


FIG. 4 (color online). Fit results and BES data for $J/\psi \to \phi\pi^+\pi^-$, $J/\psi \to \phi K^+K^-$, $J/\psi \to \omega\pi^+\pi^-$ and $J/\psi \to \omega K^+K^-$. The datapoints are uncorrected for background and detection efficiency, and the errorbars represent the statistical error. The direct $S$-wave contribution from the BES PWA and the estimated background are denoted by the dashed and dotted histographs, respectively. The solid and dashed curves describe "Fit I" and "Fit II" to the $S$-wave contributions. As described in the text, "Fit III" is performed for a fixed value of $L_6^r$ and "Fit IV" for a fixed value of $L_4^r$. The fitted parameter values are given for each case in Table I. As discussed in Sec. III D, the $J/\psi \to \omega K^+K^-$ spectrum is not included in the fits.

study of meson-meson phase shifts alone. Also, the difference between "Fit I" and "Fit II" is negligible in the $\omega\pi^+\pi^-$ spectrum.

Finally, the observed excess of events in the left wing of the $f_0(980)$ resonance in the $\phi\pi^+\pi^-$ spectrum should be mentioned, which indicates a significant presence of a nonstrange, or $\sigma$ contribution. Indeed, the fitted value of $\lambda_\phi \sim 0.13$ given in Table I reproduces this feature well.

### D. Fit results for $\omega\pi^+\pi^-$ and $\omega K^+K^-$

The most conspicuous features in $\omega\pi^+\pi^-$ are the lack of a significant peak at the position of the $f_0(980)$ resonance, and a very prominent $\sigma$ peak around a dipion energy of $\sim$0.5 GeV. It is evident that "Fit I" in the lower left-hand plot in Fig. 4 faithfully reproduces both of these features. The $\sigma$ peak is generated by the dominance of the pion nonstrange FF, which in contrast to the strange one

approaches a constant value at low energies. The main difference between the $S$-wave contribution of the BES PWA and the present fit is close to the $K\bar{K}$ threshold, where the fitted spectrum is sharply cut off by channel-coupling effects, producing a plateaulike appearance close to the $f_0(980)$ resonance. This characteristic shape is produced here by the interplay of the strange and nonstrange scalar FFs close to the $K\bar{K}$ threshold. It should also be noted that most of the remaining $\pi\pi$ events below the $K\bar{K}$ threshold are, as elaborated in Sec. III B, due to interference effects with the $b_1(1235)$ and $\rho(1450)$ resonances in the $\omega\pi$ system.

Once the parameters $L_i^r$, $\tilde{C}_\phi$ and $\lambda_\phi$ are fixed by a fit to the $\phi\pi^+\pi^-$, $\omega\pi^+\pi^-$ and $\phi K^+K^-$ spectra, the scalar FFs can be used to predict the $S$-wave contribution in the $\omega K^+K^-$ channel. It turns out that such a prediction is quite robust, since attempts at tweaking the fit by forcing changes in the $\omega K^+K^-$ sector do not have any appreciable effect. Nevertheless, it is immediately apparent from Fig. 4 that the $S$-wave contribution reported by the BES collaboration does not compare favorably with the present results. The $S$-wave fitted by BES contributes $\sim$50 events close to the $K\bar{K}$ threshold, whereas the present prediction can account for $\sim$20 events. This number can be motivated

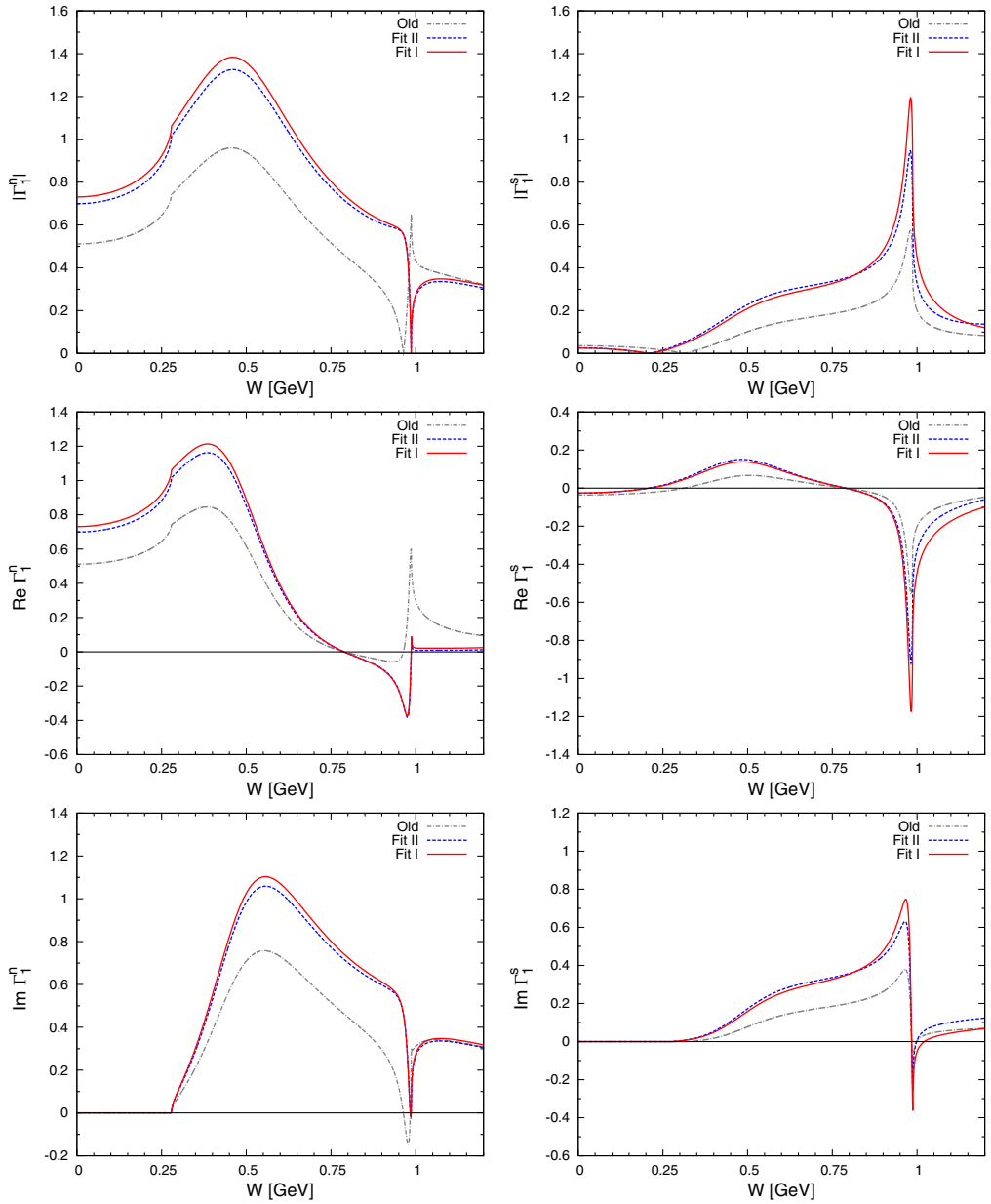


FIG. 5 (color online). The nonstrange and strange scalar FFs $\Gamma_1^n$ and $\Gamma_1^s$ of the pion. Moduli, real and imaginary parts are shown for the parameters corresponding to "Fit I" and "Fit II" in Table I. The curves labeled "Old" show, for comparison, the scalar FFs for the parameters obtained in the analysis of Ref. [7].

from the present considerations as follows: From Figs. 5 and 6, the moduli of the nonstrange pion and kaon FFs are seen to be approximately equal in magnitude, such that a roughly similar $S$-wave contribution would be expected at $\sim$1.1 GeV in the $\omega\pi^+\pi^-$ and $\omega K^+K^-$ spectra. This would lead one to expect $\sim$50 events in the $\omega K^+K^-$ spectrum as well, however the detection efficiency reported by BES for $\omega K^+K^-$ is only about half of that reported for $\omega\pi^+\pi^-$, yielding the calculated $\sim$20 events. The situation in the $\phi K^+K^-$ spectrum is different, as the modulus of the strange kaon FF at $\sim$1.1 GeV is much larger than that of the strange pion FF, as evidenced by Figs. 5 and 6.

With respect to this discrepancy, it should be noted that when the BES PWA was done, no reliable information was available on the magnitude of a possible $\sigma$ coupling to $K\bar{K}$, and therefore it was fitted freely in that analysis. The BES data exhibits interference between $\sigma \to K\bar{K}$ and a signal fitted as $K_1(1945) \to \omega K$. It turns out that the latter can be adjusted slightly in mass and width in order to reduce the $\sigma \to K\bar{K}$ signal to a level consistent, within statistical and systematical errors, with the findings of the analysis pre-

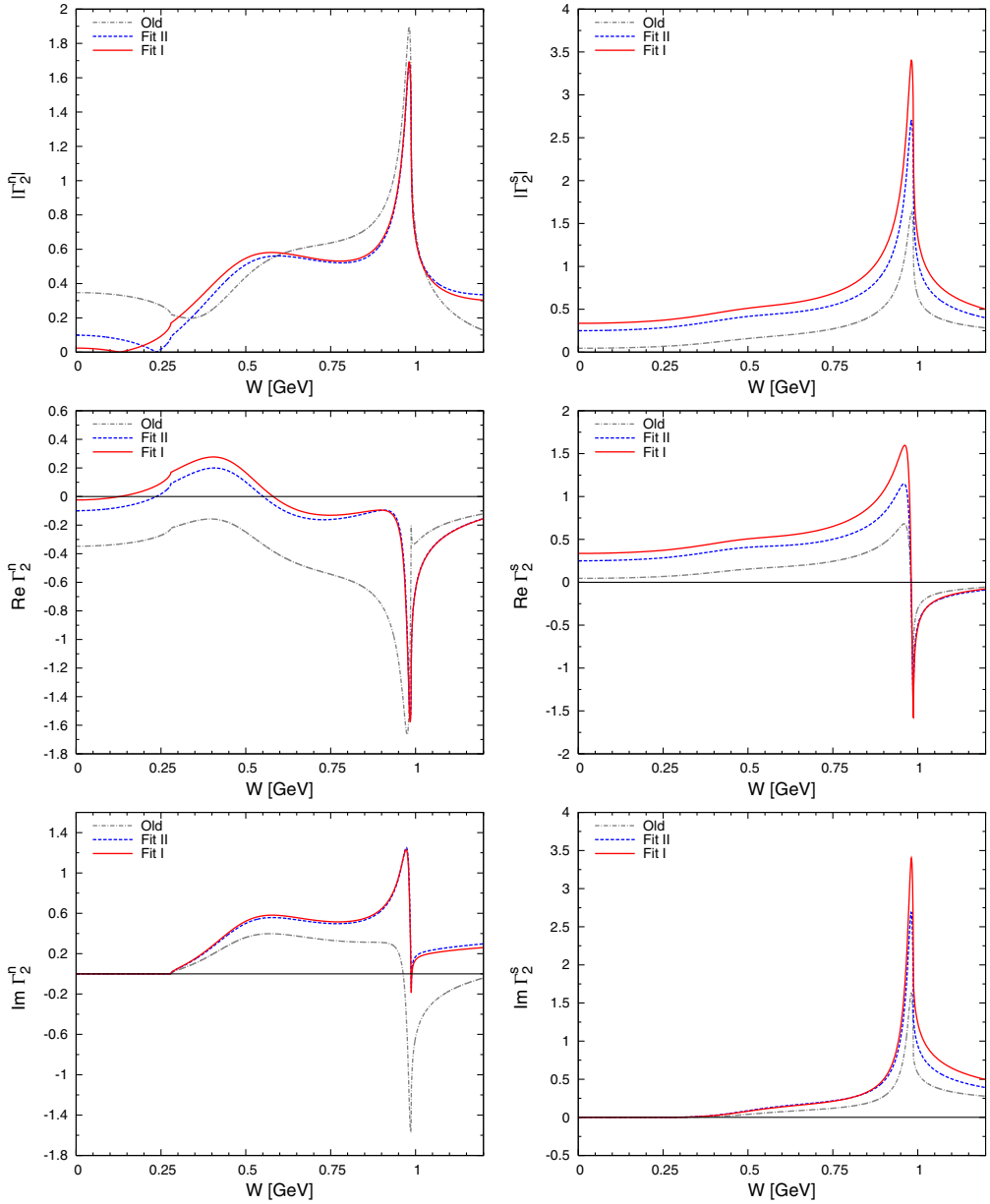


FIG. 6 (color online). The nonstrange and strange scalar FFs $\Gamma_2^n$ and $\Gamma_2^s$ of the kaon. Moduli, real and imaginary parts are shown for the parameters corresponding to "Fit I" and "Fit II" in Table I. The curves labeled Old show, for comparison, the FFs for the parameters obtained in the analysis of Ref. [7].

sented in this paper, at the price of a slightly worse fit to the $K\bar{K}$ event distribution.[2] The overall changes induced in the BES PWA by such modifications are very small.

### E. Analysis of the $L_i^r$

One of the main objectives of this analysis is the determination of the LECs $L_4^r$ and $L_6^r$, for which the data + PWA provided by the BES collaboration is certainly precise enough. As discussed in Refs. [17,35], where a set of standard estimates for the LECs of CHPT are given, $L_4^r$ and $L_6^r$ are expected, in terms of large $N_c$ arguments, to vanish at some unknown scale in the resonance region of QCD, conventionally taken to be $m_\rho$ or $m_\eta$. As discussed above, "Fit I", as given in Table I is considered the main result in this respect. The values so obtained, $(0.84 \pm 0.06) \times 10^{-3}$ for $L_4^r$ and $(0.03 \pm 0.16) \times 10^{-3}$ for $L_6^r$ should be compared with the NNLO CHPT analyses of Refs. [32,33,36], where the $L_i^r$ were extracted by fits to the available experimental data on $K_{l4}$ decays. In that study, constraints on $L_4^r$ and $L_6^r$ were also derived by requiring a properly convergent behavior of the chiral expansion up to NNLO for several quantities, such as the pseudoscalar meson masses and decay constants. It was found that such a constraint can only be satisfied in a rather small region centered around $L_4^r = 0.2 \times 10^{-3}$ and $L_6^r = 0.5 \times 10^{-3}$. Also of interest in this context is the analysis based on QCD sum rules in Ref. [37], where $L_6^r$ was constrained to be positive and in the region $0.2 \times 10^{-3} \leq L_6^r \leq 0.6 \times 10^{-3}$. Also, a significantly positive value of $L_4^r = 0.4 \times 10^{-3}$ was obtained in Ref. [37], although with unknown error. Some updated results for the $L_i^r$ are given in Ref. [38], and a recent analysis of $\pi\pi$ and $\pi K$ scattering is presented in Ref. [39], where the preferred values of $L_4^r$ and $L_6^r$ were found to be compatible with zero. Further recent determinations of the $L_i^r$ include the analyses of Refs. [29,30,40] in terms of the Inverse Amplitude Method (IAM) of Ref. [41]. In Ref. [40], a simultaneous fit to the $\pi\pi$ and $K\bar{K}$ partial-wave amplitudes for $I = 0, 1, 2$ was performed using the complete NLO CHPT amplitudes, which yielded a value of $L_4^r$ equal to $(0.2 \pm 0.1) \times 10^{-3}$. The analysis of Ref. [30] considered all two-meson scattering amplitudes including the $\eta\eta$ channel within the chiral IAM framework, which enabled the simultaneous extraction of the LECs $L_1^r$ through $L_8^r$, the reported values of $L_4^r$ and $L_6^r$ being $(-0.36 \pm 0.17) \times 10^{-3}$ and $(0.07 \pm 0.08) \times 10^{-3}$, respectively. Finally, Lattice QCD also offers the possibility of determining the LECs of CHPT via application of Partially Quenched (PQ) Lattice QCD and PQCHPT. For a theoretical background, see Refs. [42–46], and some recent Lattice QCD results for the $L_i^r$ can be found in Refs. [47–49].

[2]The authors thank David Bugg for his kind cooperation in investigating the discrepancy between the predicted $\omega K^+K^-$ spectrum and the BES analysis.

### F. Results for $L_4^r$

The value of $L_4^r$ preferred by the present study is $(0.84 \pm 0.06) \times 10^{-3}$, which is largely consistent with the value $(0.71 \pm 0.11) \times 10^{-3}$ reported in Ref. [7] where a similar analysis was performed, although with much poorer data and without the guidance of a comprehensive PWA. These results are about twice as large as the largest values found by the other analyses presented above. Also, the present result for $L_4^r$ is difficult to reconcile with the IAM analysis of Ref. [30], where a rather large but negative value of $L_4^r \sim -0.4 \times 10^{-3}$ was obtained. However, the results of that IAM analysis are not very sensitive to the value of $L_4^r$, since it has been pointed out in Ref. [31] that values of $L_4^r \sim 0$ or $L_4^r \sim 0.2 \times 10^{-3}$ can be accommodated with small overall changes.

The present value of $L_4^r$ is constrained by a simultaneous fit to the $\phi\pi^+\pi^-$ and $\omega\pi^+\pi^-$ spectra. Even a modest deviation from the central value of $L_4^r$ tends to upset the interference between the strange and nonstrange FFs at the $f_0(980)$ peak, producing for large deviations a pronounced cusp in the $\omega\pi^+\pi^-$ spectrum which contradicts the flat, plateaulike behavior seen in the experimental data. Nevertheless, the $\omega\pi^+\pi^-$ spectrum is not pathologically sensitive to the exact properties of the $f_0(980)$ resonance, since the bins centered on that energy in $\omega\pi^+\pi^-$ have been excluded from the fit; Rather, a smaller value of $L_4^r$ as used for "Fit IV", starts to upset the behavior of the low-energy parts of both the $\phi\pi^+\pi^-$ and $\omega\pi^+\pi^-$ spectra. It is thus encouraging to note that once $L_4^r$ is allowed to adjust itself optimally such that the low-energy region is well described, then the $\omega\pi^+\pi^-$ spectrum also "finds" the right shape at the $K^+K^-$ threshold. The conclusion is therefore that a smaller value of $L_4^r$ cannot easily be accommodated within the present analysis. Since the OZI rule is also based on large $N_c$ arguments, a large value of $L_4^r$ may be interpreted as a clear signal of OZI violation. However, it should be emphasized here that the inclusion of higher-order terms in the vertex of Eq. (1) may affect the value of $L_4^r$ significantly, although as discussed in Sec. III J there is little evidence as yet for such higher-order contributions.

### G. Results for $L_6^r$

For $L_6^r$, the value $(0.03 \pm 0.16) \times 10^{-3}$ determined from "Fit I" is in much better agreement with the results of the other analyses above. In remarkable contrast to the situation for $L_4^r$, the present value of $L_6^r$ is completely consistent with that determined by the IAM method in Ref. [30]. Although the present result is consistent with zero within errors, a fixed value of around $0.2 \times 10^{-3}$, as suggested by the bounds on $L_6^r$ derived in Ref. [37], does little to upset the agreement with experiment, as indicated by "Fit III", the main effect being a slight overprediction close to the $f_0(980)$ resonance in the $\omega\pi^+\pi^-$ spectrum.

As already noted in Sec. III C, the $f_0(980)$ as generated by the FSI is slightly too pronounced in the present framework, which may be interpreted as pulling the fit toward lower values of $L_6^r$. Anyway, as the main sensitivity to $L_6^r$ lies in the region of the $f_0(980)$ resonance, it is unfortunate that the presently available version of the BES PWA does not take into account channel-coupling effects for that state. If the bins of $\omega\pi^+\pi^-$ data around the $f_0(980)$ could be included in the fit, the uncertainty on $L_6^r$ would most likely be much reduced. The value of $L_6^r$ found by the old analysis in Ref. [7] is $-0.22 \times 10^{-3}$, without any error specified, which is inconsistent with the lower bound given in Ref. [37]. However, the basic reason such a value was obtained is that the $\omega\pi^+\pi^-$ spectrum was assumed, due to the lack of a PWA, to be completely dominated by the $S$-wave contribution at low energies. However, this may only constitute about $\sim$60% of the total event count, as indicated by the recent BES PWA. For this reason, the $\omega\pi^+\pi^-$ spectrum as given in Ref. [7] does not have the proper shape close to the $K\bar{K}$ threshold.

### H. Results for $L_5^r$ and $L_8^r$

The values of $L_5^r$ and $L_8^r$ are much less controversial, as most studies are in reasonable agreement concerning their numerical values. In the previous work of Ref. [7] their values were kept fixed and were taken to coincide with those determined by the $K_{l4}$ analysis of Ref. [36]. These values were quoted as $L_5^r = (0.65 \pm 0.12) \times 10^{-3}$ and $L_8^r = (0.48 \pm 0.18) \times 10^{-3}$, respectively. However, in the present analysis it turns out to be possible to let these parameters adjust themselves to their optimal values. From "Fit I" presented in Table I, the obtained values are $L_5^r = (0.45 \pm 0.09) \times 10^{-3}$ and $L_8^r = (0.33 \pm 0.17) \times 10^{-3}$. Although they come out slightly smaller than the values of Ref. [36], it is encouraging to note that an optimal fit to data does not require extreme values of $L_5^r$ and $L_8^r$. The more recent fit in Ref. [38] has reported an updated set of LECs which compare slightly more unfavorably with the present values, namely $L_5^r = (0.91 \pm 0.15) \times 10^{-3}$ and $L_8^r = (0.62 \pm 0.20) \times 10^{-3}$. However, it should be kept in mind that the nature of the fits in Ref. [38] did not allow for a detailed consideration of the effects of the LECs $L_4^r$ and $L_6^r$. It should also be noted that the values for $L_5^r$ and $L_8^r$ obtained in Refs. [36,38] are significantly smaller, and therefore in much better agreement with the present results, than the old standard values $L_5^r = (1.4 \pm 0.5) \times 10^{-3}$ and $L_8^r = (0.9 \pm 0.3) \times 10^{-3}$ in Ref. [35]. Finally, it should be noted that the results of the IAM analysis of Ref. [30] for $L_5^r$ and $L_8^r$ are essentially identical to the standard ones given in Ref. [35].

### I. Fitted values for $\tilde{C}_\phi$ and $\lambda_\phi$

The overall normalization constant $\tilde{C}_\phi$ is determined by the present analysis to be around 40 keV$^{-1/2}$, as indicated in Table I. This value is difficult to compare with Ref. [7], as that work did not consider the detection efficiencies of the DM2 and MARK-III experiments. Furthermore, Ref. [7] also employed a different definition of the overall normalization factor. In the present study, the dimension of $\tilde{C}_\phi$ is a consequence of the absorption of the proportionality factor in Eq. (15) into the product $\sqrt{2}gB_0C_\phi$. This factor could be estimated once a conversion of the event distributions reported by the BES collaboration to differential branching fractions is available. However, such an estimate is complicated by the nontriviality of the detection efficiencies shown in Fig. 3, and by a considerable uncertainty in the hitherto published values for the relevant branching fractions [34]. In principle, $\tilde{C}_\phi$ could then be used, as in Ref. [8] to extract a value for the dimensionless product $gB_0$. A determination of the coupling constant $g$ itself is more difficult since the precise value of $B_0$, which is related to the quark condensate, is only approximately known. In view of the above issues, further analysis of $\tilde{C}_\phi$ is beyond the scope of this paper.

Of considerably more interest is the fitted value of the parameter $\lambda_\phi$, which directly measures the OZI violation in the $J/\psi \to \phi\pi^+\pi^-$ and related decays. From "Fit I" in Table I, the present value is $\lambda_\phi = 0.13 \pm 0.02$, which is lower than the value $0.17 \pm 0.06$ obtained in Ref. [7], although both values are consistent given the rather large errors of the latter result. The reason for this apparent decrease in $\lambda_\phi$ can be immediately understood in terms of Eq. (8), if one notes that all of the events in the low-energy part of the $\omega\pi^+\pi^-$ spectrum were taken in Ref. [7] to be $S$-wave events. Put another way, the $S$-wave contribution for $\omega\pi^+\pi^-$ was taken to be about 50% larger in Ref. [7] than it was found to be in the BES PWA. A larger value of $\tilde{C}_\omega$ was thus required, in turn yielding a larger value of $\lambda_\phi$ via Eq. (8). Nevertheless, the present value of $\lambda_\phi$ indicates a significant amount of OZI violation, which manifests itself as a contribution to $\phi\pi^+\pi^-$ from the nonstrange scalar FF, and a contribution to $\omega\pi^+\pi^-$ from the strange one. In particular, a realistic description of the $\omega\pi^+\pi^-$ spectrum close to the $K\bar{K}$ threshold requires an interplay between the nonstrange and strange scalar FFs.

In this context, it is useful to recall Ref. [8], where the experimental results of Refs. [9–11] were normalized using the available information [34] on the width and branching fractions of the $J/\psi$. Since Ref. [8] considered only the LO CHPT contributions to the operators $\bar{n}n$ and $\bar{s}s$, the values of the $L_i^r$ do not appear as additional parameters in that model. It should be pointed out though, that the FSI between pairs of pions and kaons was taken into account in a similar way as in Ref. [7] and in the present work. Furthermore, the strength of the sequential decay mechanism via intermediate vector and axial-vector resonances could be fixed from experimental information [34] up to a relative sign of the respective coupling constants. Up to

this relative sign, the only free parameters in the calculation of Ref. [8] were $gB_0$ and $\lambda_\phi$. The sign ambiguity could not be resolved in Ref. [8], since equally good fits to the data were obtained for both choices. If both the $J/\psi \to VP$ and $J/\psi \to AP$ coupling constants have the same sign, Ref. [8] finds $gB_0 = 0.032 \pm 0.001$ and $\lambda_\phi = 0.12 \pm 0.03$. This value of $\lambda_\phi$ is consistent with the one obtained from "Fit I" in Table I.

### J. Results for the scalar form factors

Once all parameters are determined by the analysis of the BES data [12–14], the shapes and magnitudes of the scalar FFs of the pion and the kaon are fixed. In Figs. 5 and 6, they are shown for the fitted parameters given in Table I and compared to the form factors obtained in Ref. [7]. It is evident that the values of the form factors at the origin have changed significantly with respect to those of Ref. [7], even though the gross features remain similar. The most significant change is that the form factors now have a realistic behavior close to the $K\bar{K}$ threshold, which is reflected in the values of the form factors at the origin. Thus $\Gamma_1^n(0)$ has increased by $\sim$30%, while the value of $\Gamma_1^s(0)$ remains very small and negative. The situation for the kaon form factors is more drastic, since they were not very well determined in Ref. [7]. The present results indicate that $\Gamma_2^n(0)$ is small and negative, while $\Gamma_2^s(0)$ is positive and has increased significantly from the value determined by previous work.

Since the description of the experimental data shown in Fig. 4 is satisfactory, a natural question to ask is whether the scalar FFs can be considered realistic as well. The issue is complicated by the essentially unknown momentum dependence of the vertex given in Eq. (1), for which the simplest possible form was assumed in Ref. [7]. The question is then whether the scalar FFs are simulating some neglected momentum-dependence in the $J/\psi \to \phi$ and $J/\psi \to \omega$ vertices. Although the detailed study of this is beyond the scope of the present study, the scalar radius $\langle r^2\rangle_s^\pi$ of the pion and the curvature $c_s^\pi$ of the nonstrange scalar FF may nevertheless be used to check for consistency with other theoretical descriptions. These quantities are defined [18,50] in terms of the expansion

$$\frac{\Gamma_\pi^n(s)}{\Gamma_\pi^n(0)} = 1 + \frac{1}{6}\langle r^2\rangle_s^\pi s + c_s^\pi s^2 + \mathcal{O}(s^3), \qquad (42)$$

of the nonstrange scalar FF of the pion around $s = 0$. The values for $\langle r^2\rangle_s^\pi$ given by "Fit I" in Table I are quite stable around $0.657 \pm 0.006$ fm$^2$, whereas the values for $c_s$ are $\sim$12.50 GeV$^{-4}$ for "Fit I" and $\sim$12.53 GeV$^{-4}$ for "Fit II". These values can be compared with other theoretical predictions, starting from the prediction of Ref. [17], where an estimate of $\langle r^2\rangle_s^\pi = 0.55 \pm 0.15$ fm$^2$ was obtained from the experimental value of $F_K/F_\pi$, neglecting OZI-violating contributions. This estimate has been refined by the dispersive work of Ref. [51] and further improved upon in Ref. [52] using the $\pi\pi$ Roy equations to yield $\langle r^2\rangle_s^\pi = 0.61 \pm 0.04$ fm$^2$. In Ref. [51], the curvature $c_s^\pi$ was also determined and found to be around $\sim$10.6 GeV$^{-4}$, which is about 10% smaller than the present value. In the NNLO CHPT analysis of Ref. [33], the value of $c_s^\pi$ could not be pinned down very precisely, although the preferred values are in the range $10 \ldots 13$ GeV$^{-4}$.

The effects of inelasticities due to the $\pi\pi \to 4\pi$ and $\pi\pi \to \eta\eta$ channels were studied in detail in Ref. [37], which produced a range of values for $\langle r^2\rangle_s^\pi$ consistent with the result of Ref. [52]. Higher-order CHPT corrections to the scalar FFs have been considered in Ref. [50] and in the NNLO fits of Refs. [32,33], which also yielded a preferred value of $\langle r^2\rangle_s^\pi$ around $\sim$0.61 fm$^2$. Finally, the value of $\langle r^2\rangle_s^\pi$ has also been extracted from the $S$-wave $\pi\pi$ phase shift for $I = 0$ using the sum rule of Ref. [53], which yielded a value of $0.75 \pm 0.07$ fm$^2$. However, as stated in Ref. [54], this work is not in agreement with earlier determinations of $\langle r^2\rangle_s^\pi$.

The conclusion of this comparison is that the present values for the pion scalar radius $\langle r^2\rangle_s^\pi$ and the curvature $c_s^\pi$ of the pion scalar FF are largely consistent with other recent theoretical descriptions. The present $\langle r^2\rangle_s^\pi$ value of $\sim$0.65 fm$^2$ is at the upper limit of the generally accepted value of $0.61 \pm 0.04$ fm$^2$. It is possible that the slightly higher value found in the present study is hinting at a neglected momentum dependence in the vertex of Eq. (1) or at some inaccuracy in the present description of the $\pi\pi$ phase shifts. Nevertheless, the reasonable value of $\langle r^2\rangle_s^\pi$ is reassuring in view of the somewhat unorthodox value of $L_4^r$ obtained from the present analysis.

## IV. DISCUSSION AND OUTLOOK

The main results of this analysis of the experimental BES results [12–14] are the set of values obtained for the $L_i^r$ and the corresponding sets of scalar FFs of the pions and kaons. Because of the accuracy of the BES data, the actual errors of the $L_i^r$ are dominated by the uncertainty in the theoretical description. The present value of $L_6^r$ is small and compares well with the known theoretical bounds. The present value is compatible with zero, although on the positive side. On the other hand, $L_4^r$ was found to be large and positive, around $(0.84 \pm 0.06) \times 10^{-3}$. It has also been shown that a value of $L_4^r$ smaller than about $0.7 \times 10^{-3}$ is not compatible with the present analysis. Although this value of $L_4^r$ is in conflict with most of the presently available fits of the $L_i^r$, an advantage of the present analysis is that the expressions for the scalar FFs depend on only four LECs, namely $L_4^r$, $L_5^r$, $L_6^r$ and $L_8^r$, and that no assumptions about their values had to be made, since all of them could be constrained in a unique way. Also, it should be kept in mind that the present description of the scalar FFs, although certainly not complete, contains some of the features that would be present in an all-orders calculation in CHPT. In contrast, determinations of the $L_i^r$ from trun-

cated NLO or NNLO CHPT expansions suffer from possibly large errors due to the neglect of higher-order contributions, and the poorly known values of the NNLO LECs.

Naturally, a further question to ask is whether the fitted value of $L_4^r$ could be modified by changing some of the features of the present description of the $J/\psi$ decays; Possible avenues of further investigation include the consideration of the $\eta\eta$ channel in the FSI which was neglected in this work, although it cannot be argued that this is necessarily a large effect as the description of the FSI is independent of the $L_i^r$ at this level of theoretical sophistication. It should also be noted that in the IAM framework of Ref. [41], the $\pi\pi$ phase shift is given in terms of the $L_i^r$, and thus more flexibility of adjustment is possible. On the other hand, such an approach may actually turn out to be more constraining than the present one, since the pole position of the $f_0(980)$ resonance is then directly affected by the $L_i^r$.

Another essentially open question is whether a more relevant decay vertex than the one given in Eq. (1) should be considered or not. In order to give a partial answer to this question, the pion scalar radius has been estimated for the present set of scalar FFs. If the FFs were compensating heavily for some neglected momentum dependence in the $J/\psi \to \phi$, $\omega$ vertex, this might reveal itself as an unrealistic value for $\langle r^2\rangle_s^\pi$. The present analysis gives a value close to $\sim 0.65$ fm$^2$ which, as argued in Sec. III J, is in reasonable agreement with other recent theoretical predictions. It therefore appears that there is no compelling evidence as yet for a significant momentum dependence in the vertex described here by Eq. (1).

An issue often raised is the different appearance of the dipion spectra in the $\omega\pi\pi$ and $\phi\pi\pi$ channels, which are shown in Fig. 4. Within the present framework, this difference can be understood in very simple terms. According to the expectations from the OZI rule, the $\omega\pi\pi$ spectrum should be dominated by the nonstrange scalar FF of the pion, whereas the $\phi\pi\pi$ process should essentially be driven by the strange scalar FF alone. However, the latter one vanishes to LO in CHPT, which leads to a strong suppression of the low-energy tail of the dipion spectrum in $\phi\pi\pi$. On the other hand, the nonstrange FF is nonzero to LO in CHPT, and thus the decay amplitude itself does not vanish for low dipion energies in the $\omega\pi\pi$ decay. The appearance of the experimental $\omega\pi\pi$ spectrum near the $\pi\pi$ threshold is then given by the squared modulus of the nonstrange scalar FF and phase space.

In this context the OZI violation parameter $\lambda_\phi$ is instructive, since it determines whether any contribution from the nonstrange pion scalar FF is present in the $\phi\pi\pi$ decay process. It turned out that $\lambda_\phi$ could be quite accurately determined from the present fits, which yielded a value of $\lambda_\phi = 0.13 \pm 0.02$, which indicates that the nonstrange pion scalar FF contributes significantly to the $\phi\pi\pi$ decay, and indeed this contribution appears as a distinct enhancement in the low-energy tail of the dipion distribution shown in Fig. 4. Nevertheless, this parameter has decreased from the old value of around $\lambda_\phi \sim 0.17$ given in Ref. [7], due to the fact that the $S$-wave $\sigma$ contribution to the $\omega\pi\pi$ decay has turned out to be smaller than previously estimated. As discussed in Sec. III I, the present value of $\lambda_\phi$ is consistent with that obtained in Ref. [8], where the strong interaction in the $\omega\pi$ and $\phi\pi$ systems was explicitly taken into account. This was not done in the present work since a determination of the direct $S$-wave contribution via PWA is available [12–14].

An extra bonus of the present work is that the dikaon distribution in the $\omega K^+K^-$ decay could be predicted close to the $K\bar{K}$ threshold, which is instructive since the present experimental data for that channel is difficult to interpret in terms of a PWA [14]. In the same way, the predicted shape of the $S$-wave distribution in the $\omega\pi^+\pi^-$ decay is slightly different from the one favored by the BES PWA. Finally, as the scalar FFs of the pion and the kaon have been strongly constrained by the $J/\psi$ decays analyzed in this paper, the impact of these newly determined scalar FFs can be studied for other processes like $B \to \sigma\pi$ [55] or $B$ decays into three pseudoscalars, such as $B \to K_S^0\pi\pi$ [56]. Work along these lines is under way.

## ACKNOWLEDGMENTS

This research is part of the EU Integrated Infrastructure Initiative Hadron Physics Project under contract number RII3-CT-2004-506078 and DFG (SBF/TR 16, ''Subnuclear Structure of Matter''). The authors thank David Bugg and Liaoyuan Dong for their invaluable assistance in making the BES data available. T. L. thanks Bachir Moussallam, Leonard Leśniak, José Oller and José Peláez for email correspondence, and Johan Bijnens for assistance with the scalar FFs in CHPT, and Christoph Hanhart and Udit Raha for instructive discussions. T. L. is grateful to Bastian Kubis for sharing unpublished results on issues relevant to this paper. T. L. acknowledges a travel stipend from the Mikael Björnberg memorial foundation.

[1] K. L. Au, D. Morgan, and M. R. Pennington, Phys. Rev. D **35**, 1633 (1987); D. Morgan and M. R. Pennington, Phys. Rev. D **48**, 1185 (1993); **48**, 5422 (1993).

[2] J. D. Weinstein and N. Isgur, Phys. Rev. Lett. **48**, 659 (1982); Phys. Rev. D **27**, 588 (1983); **41**, 2236 (1990).

[3] G. Janssen, B. C. Pearce, K. Holinde, and J. Speth, Phys. Rev. D **52**, 2690 (1995).

[4] S. Okubo, Phys. Lett. **5**, 165 (1963); G. Zweig, CERN Report No. CERN-TH-401; CERN Report No. CERN-TH-412 (unpublished); J. Iizuka, Prog. Theor. Phys. Suppl. **37**, 21 (1966); J. Iizuka, K. Okada, and O. Shito, Prog. Theor. Phys. **35**, 1061 (1966).

[5] G. 't Hooft, Nucl. Phys. **B72**, 461 (1974); E. Witten, Nucl. Phys. **B160**, 57 (1979).

[6] N. Isgur and H. B. Thacker, Phys. Rev. D **64**, 094507 (2001).

[7] Ulf-G. Meißner and J. A. Oller, Nucl. Phys. A **679**, 671 (2001).

[8] L. Roca, J. E. Palomar, E. Oset, and H. C. Chiang, Nucl. Phys. A **744**, 127 (2004); Int. J. Mod. Phys. A **20**, 1897 (2005).

[9] A. Falvard *et al.* (DM2 Collaboration), Phys. Rev. D **38**, 2706 (1988).

[10] W. S. Lockman (MARK-III Collaboration), Report No. SLAC-PUB-5139.

[11] N. Wu, hep-ex/0104050.

[12] M. Ablikim *et al.* (BES Collaboration), Phys. Lett. B **607**, 243 (2005).

[13] M. Ablikim *et al.* (BES Collaboration), Phys. Lett. B **598**, 149 (2004).

[14] M. Ablikim *et al.* (BES Collaboration), Phys. Lett. B **603**, 138 (2004).

[15] J. A. Oller and E. Oset, Nucl. Phys. A **620**, 438 (1997); **652**, 407(E) (1999).

[16] S. Weinberg, Physica (Amsterdam) A **96**, 327 (1979).

[17] J. Gasser and H. Leutwyler, Nucl. Phys. **B250**, 465 (1985); **B250**, 517 (1985); **B250**, 539 (1985).

[18] J. Gasser and H. Leutwyler, Ann. Phys. (N.Y.) **158**, 142 (1984).

[19] Ulf-G. Meißner, Comments Nucl. Part. Phys. **20**, 119 (1991).

[20] N. A. Törnqvist, Phys. Rev. Lett. **49**, 624 (1982); N. A. Törnqvist and M. Roos, Phys. Rev. Lett. **76**, 1575 (1996).

[21] E. Van Beveren, T. A. Rijken, K. Metzger, C. Dullemond, G. Rupp, and J. E. Ribeiro, Z. Phys. C **30**, 615 (1986).

[22] R. L. Jaffe, Phys. Rev. D **15**, 267 (1977).

[23] J. A. Oller and E. Oset, Phys. Rev. D **60**, 074023 (1999).

[24] J. A. Oller and E. Oset, Nucl. Phys. A **629**, 739 (1998).

[25] J. A. Oller, Phys. Lett. B **426**, 7 (1998); E. Marco, S. Hirenzaki, E. Oset, and H. Toki, Phys. Lett. B **470**, 20 (1999).

[26] J. A. Oller, Phys. Rev. D **71**, 054030 (2005).

[27] S. Scherer, in *Advances in Nuclear Physics*, edited by J. W. Negele and E. Vogt (Kluwer Academic/Plenum Publishers, New York, 2003), Vol. 27, pp. 277–538; G. Ecker, hep-ph/0011026; A. Pich, hep-ph/9806303.

[28] M. Benayoun, L. DelBuono, P. Leruste, and H. B. O'Connell, Eur. Phys. J. C **17**, 303 (2000).

[29] J. A. Oller, E. Oset, and J. R. Peláez, Phys. Rev. D **59**, 074001 (1999); **60**, 099906(E) (1999).

[30] A. Gómez Nicola and J. R. Peláez, Phys. Rev. D **65**, 054009 (2002).

[31] J. R. Peláez, Mod. Phys. Lett. A **19**, 2879 (2004).

[32] J. Bijnens, G. Colangelo, and P. Talavera, J. High Energy Phys. 05 (1998) 014.

[33] J. Bijnens and P. Dhonte, J. High Energy Phys. 10 (2003) 061.

[34] S. Eidelman *et al.* (Particle Data Group), Phys. Lett. B **592**, 1 (2004).

[35] J. Bijnens, G. Ecker, and J. Gasser, in *The Second DA$\Phi$NE Physics Handbook*, edited by L. Maiani, G. Pancheri, and N. Paver (INFN-LNF publications, Frascati, Italy, 1995), Vol. 1, pp. 125–144.

[36] G. Amorós, J. Bijnens, and P. Talavera, Nucl. Phys. **B585**, 293 (2000); **B598**, 665(E) (2001); Phys. Lett. B **480**, 71 (2000).

[37] B. Moussallam, Eur. Phys. J. C **14**, 111 (2000); J. High Energy Phys. 08 (2000) 005.

[38] G. Amorós, J. Bijnens, and P. Talavera, Nucl. Phys. **B602**, 87 (2001).

[39] J. Bijnens, P. Dhonte, and P. Talavera, J. High Energy Phys. 05 (2004) 036; 01 (2004) 050.

[40] F. Guerrero and J. A. Oller, Nucl. Phys. **B537**, 459 (1999); **B602**, 641(E) (2001).

[41] T. N. Truong, Phys. Rev. Lett. **61**, 2526 (1988); Phys. Rev. Lett. **67**, 2260 (1991); A. Dobado, M. J. Herrero, and T. N. Truong, Phys. Lett. B **235**, 134 (1990); J. A. Oller, E. Oset, and J. R. Peláez, Phys. Rev. Lett. **80**, 3452 (1998).

[42] A. Morel, J. Phys. (France) **48**, 1111 (1987); C. W. Bernard and M. F. L. Golterman, Phys. Rev. D **46**, 853 (1992); S. R. Sharpe, Phys. Rev. D **46**, 3146 (1992).

[43] C. W. Bernard and M. F. L. Golterman, Phys. Rev. D **49**, 486 (1994); S. R. Sharpe and N. Shoresh, Phys. Rev. D **62**, 094503 (2000); **64**, 114510 (2001).

[44] J. Bijnens, N. Danielsson, and T. A. Lähde, Phys. Rev. D **70**, 111503 (2004); **73**, 074509 (2006).

[45] J. Bijnens and T. A. Lähde, Phys. Rev. D **71**, 094502 (2005); **72**, 074502 (2005).

[46] S. Dürr, Eur. Phys. J. C **29**, 383 (2003); D. R. Nelson, G. T. Fleming, and G. W. Kilcup, Phys. Rev. Lett. **90**, 021601 (2003).

[47] J. Heitger, R. Sommer, and H. Wittig (ALPHA Collaboration), Nucl. Phys. **B588**, 377 (2000).

[48] F. Farchioni, I. Montvay, and E. Scholz (qq + q Collaboration), Eur. Phys. J. C **37**, 197 (2004).

[49] C. Aubin *et al.* (MILC Collaboration), Phys. Rev. D **70**, 114501 (2004).

[50] J. Gasser and Ulf-G. Meißner, Nucl. Phys. **B357**, 90 (1991).

[51] J. F. Donoghue, J. Gasser, and H. Leutwyler, Nucl. Phys. **B343**, 341 (1990).

[52] G. Colangelo, J. Gasser, and H. Leutwyler, Nucl. Phys. **B603**, 125 (2001).

[53] F. J. Ynduráin, Phys. Lett. B **578**, 99 (2004); **586**, 439(E) (2004); **612**, 245 (2005).

[54] B. Ananthanarayan, I. Caprini, G. Colangelo, J. Gasser, and H. Leutwyler, Phys. Lett. B **602**, 218 (2004).

[55] S. Gardner and Ulf-G. Meißner, Phys. Rev. D **65**, 094004 (2002).

[56] A. Furman, R. Kamiński, L. Leśniak, and B. Loiseau, Phys. Lett. B **622**, 207 (2005).